A Graphical and Analytical Study of $\chi(s)$ and the Localization of Zeros of the Riemann Zeta Function

AI-assisted translation from French to English by the author.

Mohammed Djamal CHEBBAH
Independent researcher
chebbah.djamel@gmail.com

Octobre 05, 2025

Abstract

This work explores new analytical properties of the auxiliary function $\chi(s)$ within the critical strip of the Riemann zeta function. By combining symmetry constraints derived from the functional equation with domain exclusion principles, we identify regions where non-trivial zeros of $\zeta(s)$ cannot occur.

We employ three complementary tools — graphical visualization, analytical arguments, and numerical computations — leading to two convergent results that map the critical strip and precisely characterize the region where the zeta function may vanish. The systematic elimination of excluded regions highlights the critical line $\Re(s) = \frac{1}{2}$ as the remaining domain of interest.

These results provide new insights into the distribution of zeros of the Riemann zeta function and offer a systematic framework that could be applied to related problems in analytic number theory

Keywords

Riemann zeta function, χ function, non-trivial zeros, Riemann Hypothesis, zeros in the critical strip, analytic number theory.

Acknowledgments

I would like to express my deep gratitude to all those who have contributed to the completion of this work, whether through their encouragement, enlightening discussions, or benevolent support.

1 Introduction

1.1 Riemann Zeta Function

The Riemann zeta function [1, p. 1], [2, p. 9, § 1.4], [3, p. 1, § 1.1], is a complex function of the variable $s = \sigma + it$, where σ and t are real, defined for $\sigma > 1$ by the Riemann series:

$$\zeta(s) = \sum_{n=1}^{\infty} \frac{1}{n^s} \tag{1}$$

Through analytic continuation [1, pp. 2-3], [3, p. 13, § 2.1], Riemann succeeded as early as 1859 in connecting this function to the prime-counting function $\pi(x)$, which gives the number of primes less than or equal to a given value x. This connection relies particularly on the knowledge of the *non-trivial zeros* of $\zeta(s)$, that is, the solutions of the equation $\zeta(s) = 0$ located in the *critical strip* $0 \leq \Re(s) \leq 1$.

1.2 Riemann Hypothesis

In his paper [1, p. 5], Riemann conjectured that all non-trivial zeros of the function $\zeta(s)$ in the critical strip lie on the *critical line* $\sigma = \frac{1}{2}$. To this day, this hypothesis has been neither refuted nor confirmed. This work explores properties of the auxiliary $\chi(s)$ function that lead to new constraints on the location of non-trivial zeros of $\zeta(s)$. A detailed development of this approach is presented in the following sections..

1.3 Review of Fundamental Relations for the Zeta Function

1.3.1 The $\zeta(s)$ Function

Conjugation of $\zeta(s)$, [3, p. 1, § 1.1]:

$$\zeta(s) = \overline{\zeta(\bar{s})} \tag{2}$$

and

$$|\zeta(s)| = |\zeta(\bar{s})|.$$

The analytic continuation of the ζ function to $\mathbb{C} \setminus \{1\}$, introduced by Riemann [3, p. 16, Eq. 2.1.9], leads to the functional equation:

$$\zeta(s) = \chi(s)\, \zeta(1 - s). \tag{3}$$

With the value of $\chi(s)$ [3, p. 16, Eq. 2.1.10] given by:

$$\frac{\zeta(s)}{\zeta(1-s)} = \chi(s) = \frac{\pi^{s-\frac{1}{2}} \Gamma\left(\frac{1-s}{2}\right)}{\Gamma\left(\frac{s}{2}\right)}, \quad s \in \mathbb{C} \setminus \left(\{1, 3, 5, \dots\} \cup \{0, -2, -4, \dots\}\right). \tag{4}$$

Since our study is situated in the critical strip, excluding the singular points at $s = 0$ and $s = 1$, we introduce the following subdomains:

- $\mathcal{D} = \{s \in \mathbb{C} : 0 \leq \Re(s) \leq 1\} \setminus \{0, 1\}$: the complete critical strip excluding these 2 singular points.
- $\mathcal{D}^+ = \{s \in \mathbb{C} : 0 \leq \Re(s) \leq 1,\ \Im(s) > 0\} \setminus \{0\}$: the upper part of the critical strip.

From equation (3), $\zeta(s) = \chi(s)\zeta(1 - s)$, we obtain by taking moduli the relation valid everywhere in $\mathcal{D}$:

$$|\zeta(s)| = |\chi(s)| \cdot |\zeta(1 - s)|. \tag{5}$$

The conjugation of the function $\chi(s)$ follows from the conjugation of its terms:

$$\chi(s) = \overline{\chi(\bar{s})} \quad \text{and} \quad |\chi(s)| = |\chi(\bar{s})| \tag{6}$$

Given the equation $\chi(s) \cdot \chi(1 - s) = 1$, [3, p. 16, Eq. 2.1.11], $\chi(s)$ is different from 0 for all s. Hence:

$$|\chi(s)| \neq 0 \quad \text{for} \quad 0 \leq \sigma \leq 1, \quad \forall t > 0 \tag{7}$$

1.3.2 Clarifications

Common misinterpretations concerning the vanishing of both sides of the functional equation are clarified by the following remark.

Remark (Resolution of the $0/0$ and $0 = \chi(s) \times 0$ indeterminacies).

Let

$$\mathcal{D} = \{s \in \mathbb{C} : 0 < \Re(s) < 1\}$$

be the critical strip. Whenever $\zeta(1-s) \neq 0$, the functional equation $\zeta(s) = \chi(s)\zeta(1-s)$ gives

$$\frac{\zeta(s)}{\zeta(1-s)} = \chi(s).$$

Hence the quotient

$$R(s) := \frac{\zeta(s)}{\zeta(1-s)}$$

defines a holomorphic function on the open set $\mathcal{D} \setminus Z$, where $Z = \{s \in \mathcal{D} : \zeta(1-s) = 0\}$. On this set we have $R(s) = \chi(s)$. Since χ is holomorphic and non-vanishing on the whole strip $\mathcal{D}$ (by its explicit expression in terms of Gamma functions), and since $\mathcal{D} \setminus Z$ has accumulation points in $\mathcal{D}$, the identity theorem for holomorphic functions implies that R admits a unique holomorphic extension to $\mathcal{D}$, and this extension must be precisely $\chi(s)$.
In particular, at a zero s_n where $\zeta(s_n) = \zeta(1-s_n) = 0$, the value of the quotient is not a matter of convention. Since s_n and $1-s_n$ must have the same multiplicity (as $\chi(s_n) \neq 0, \infty$), the limit exists and is forced by analytic continuation:

$$\boxed{\lim_{s \to s_n} \frac{\zeta(s)}{\zeta(1-s)} = \chi(s_n).}$$

Thus the relation $0 = \chi(s_n) \times 0$ is merely an identity obtained after evaluation, not a condition determining $\chi(s_n)$. Consequently, $\chi(s_n)$ cannot assume arbitrary values as one might mistakenly think; it is uniquely determined by analytic continuation and retains the same value it has on the rest of the critical strip.

1.3.3 The $\xi(s)$ Function

The function $\xi(s)$, [1, p. 4], [3, p. 16, Eq. 2.1.1], is related to the $\zeta(s)$ function by the following relation:

$$\xi(s) = \frac{1}{2} s(s-1) \pi^{-\frac{s}{2}} \Gamma\left(\frac{s}{2}\right) \zeta(s) \tag{8}$$

The function $\xi(s)$ is holomorphic on $\mathbb{C}$, due to the factor $(s-1)$ which compensates for the pole of the $\zeta(s)$ function at $s = 1$. The function $\xi(s)$ satisfies the functional equation [3, p. 16, Eq. 2.1.13]:

$$\xi(s) = \xi(1-s) \tag{9}$$

Lemma 1.1. *In the critical strip $\mathcal{D}$, the non-trivial zeros of $\zeta(s)$ coincide exactly with those of $\xi(s)$:*

$$\xi(s) = 0 \quad \Longleftrightarrow \quad \zeta(s) = 0 \tag{10}$$

Proof. According to equation (8), for $s \neq 0$ in the critical strip, $\xi(s) = 0$ if and only if $\zeta(s) = 0$, since the other factors of $\xi(s)$ do not vanish for $0 \leq \sigma \leq 1$. The factor $(s-1)$ compensates for the pole of $\zeta(s)$ at $s = 1$, and the gamma function has no zeros.

Lemma 1.2. *In the critical strip $\mathcal{D}$, the non-trivial zeros of $\zeta(s)$ are symmetric with respect to the point $(\frac{1}{2}, 0)$.*

For any zero s_n of $\zeta(s)$ we have:

$$\zeta(s_n) = \zeta(1 - s_n) \tag{11}$$

Proof. Let s_n be a non-trivial zero of $\zeta(s)$ in the critical strip. By Lemma 1.1, $\xi(s_n) = 0$. By the functional equation $\xi(s) = \xi(1 - s)$, we have $\xi(1 - s_n) = 0$, hence $\zeta(1 - s_n) = 0$. Thus, both s_n and $1 - s_n$ are non-trivial zeros of $\zeta(s)$.

Fundamental consequence:
There cannot exist an "isolated" zero in the critical strip that would violate this symmetry.

From equation (9), we also deduce:

$$|\xi(s)| = |\xi(1 - s)| \tag{12}$$

Conjugation:

$$\xi(\bar{s}) = \overline{\xi(s)} \quad \text{and} \quad |\xi(s)| = |\xi(\bar{s})| \tag{13}$$

Symmetry of $|\xi(s)|$ with respect to the critical line $\sigma = \frac{1}{2}$:
Combining equations (12) and (13) we obtain the chain of equalities:

$$|\xi(s)| = |\xi(1 - s)| = |\xi(\overline{1 - s})|,$$

hence:

$$|\xi(s)| = |\xi(\overline{1 - s})|. \tag{14}$$

Since the points s and $\overline{1 - s}$ are symmetric with respect to the line $\sigma = \frac{1}{2}$, the function $|\xi(s)|$ is symmetric with respect to this line.

2 Methodology

2.1 Foundation

Our approach is based on the analytical framework established by Riemann for the zeta function and its associated functions, particularly the $\chi(s)$ function. We rely exclusively on classical tools from complex analysis (analytic continuation, the functional equation, properties of the Gamma function) and do not invoke conjectural results or advanced modern techniques. This self-contained approach ensures that all conclusions follow directly from established theorems

2.2 Domain Exclusion Principle

The procedure adopts a progressive exclusion strategy: by identifying regions of the critical strip where $|\chi(s)| \neq 1$, we establish that these areas cannot contain symmetric pairs of zeros. Through successive elimination, we reduce the possible domain for zeros to the critical line.

2.3 Use of Graphical Methods

Visual analysis guides intuition by revealing the geometric properties of $|\chi(s)|$ in the critical strip. Graphical representations, generated by Python scripts with Matplotlib, serve to formulate conjectures that are then demonstrated analytically.

2.4 Use of numerical certification

To confirm analytical demonstrations and their results, we have introduced numerical certifications using Arb interval arithmetic. This approach provides rigorous, computer-assisted proofs that complement the theoretical analysis. Employing high-precision interval arithmetic. eliminate any uncertainty due to floating-point approximations. The combination of symbolic reasoning and validated numerics ensures the robustness of the conclusions presented in this work.

2.5 Pedagogical Approach

The document aims to reconcile accessibility with mathematical rigor. Certain standard developments are explicitly detailed to guarantee the completeness of the reasoning and facilitate verification by the community. All graphical representations and numerical certifications are reproducible from the formulas provided.

3 Analytical Symmetries of $|\zeta|$ and $|\xi|$ in $\mathcal{D}$

To make visible the symmetries of the functions $|\xi(s)|$ and $|\zeta(s)|$, we have chosen to represent the modulus of these functions using a color scale in the complex plane, (see Figure 1 and Figure 2). This choice highlights the analytical symmetries, makes zeros identifiable, and allows for immediate visual reading of the properties of these functions.

3.1 Symmetries of the $|\xi(s)|$ Function

The function $|\xi(s)|$, defined on the complex plane, possesses a particularly rich symmetry structure (see Figure 1).

• Symmetry with respect to the real axis (σ-axis):

$$\xi(\overline{s}) = \overline{\xi(s)} \quad \Longrightarrow \quad |\xi(s)| = |\xi(\overline{s})|.$$

This means that $|\xi(s)|$ is symmetric with respect to the reflection $t \mapsto -t$, hence with respect to the axis $t = 0$.

• Central symmetry with respect to the point $\left(\frac{1}{2}, 0\right)$: Using the functional equation of $\xi(s)$, see equation (9), we obtain:

$$|\xi(s)| = |\xi(1-s)|.$$

This induces a central symmetry of $|\xi(s)|$ with respect to the critical point $\left(\frac{1}{2}, 0\right)$.

• Symmetry with respect to the critical line $\sigma = \frac{1}{2}$: this symmetry was demonstrated in Subsection 1.3.3, it is due to the fact that $|\xi(s)| = |\xi(\overline{1-s})|$.

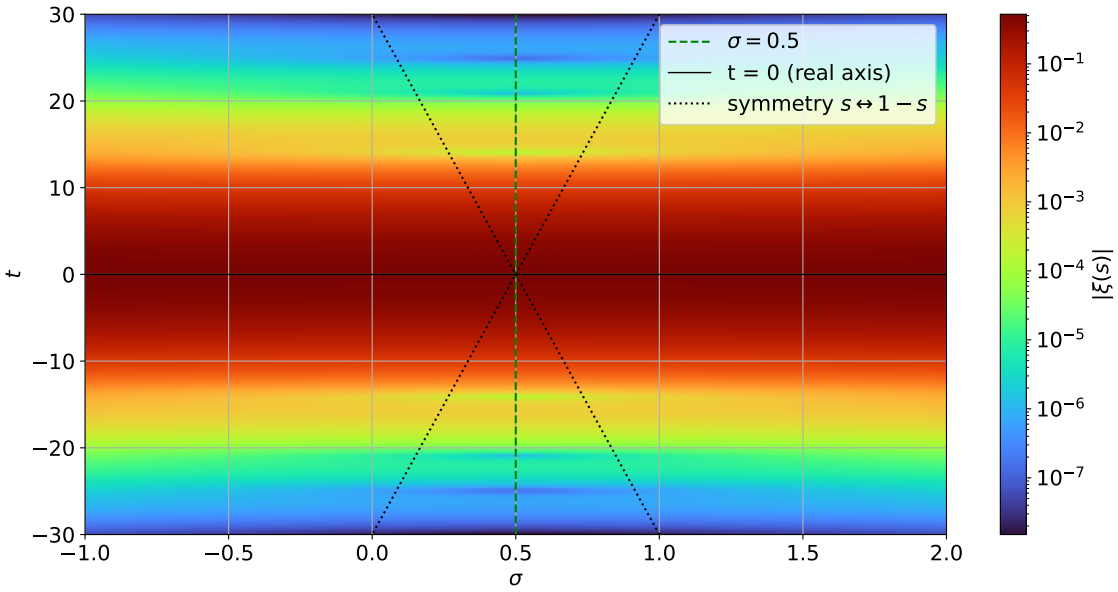

Figure 1: Symmetries of the $|\xi(s)|$ function in the complex plane

3.2 Symmetry of the $|\zeta(s)|$ Function

The function $|\zeta(s)|$, on the other hand, exhibits a more restricted symmetry structure.
• Symmetry with respect to the real axis ($t = 0$): Figure 2 shows that this unique symmetry contrasts with the triple symmetry of $|\xi(s)|$. We observe only symmetry with respect to the σ-axis, by virtue of the equality $|\zeta(s)| = |\zeta(\bar{s})|$ due to the conjugation of the $\zeta(s)$ function, see equation (2).

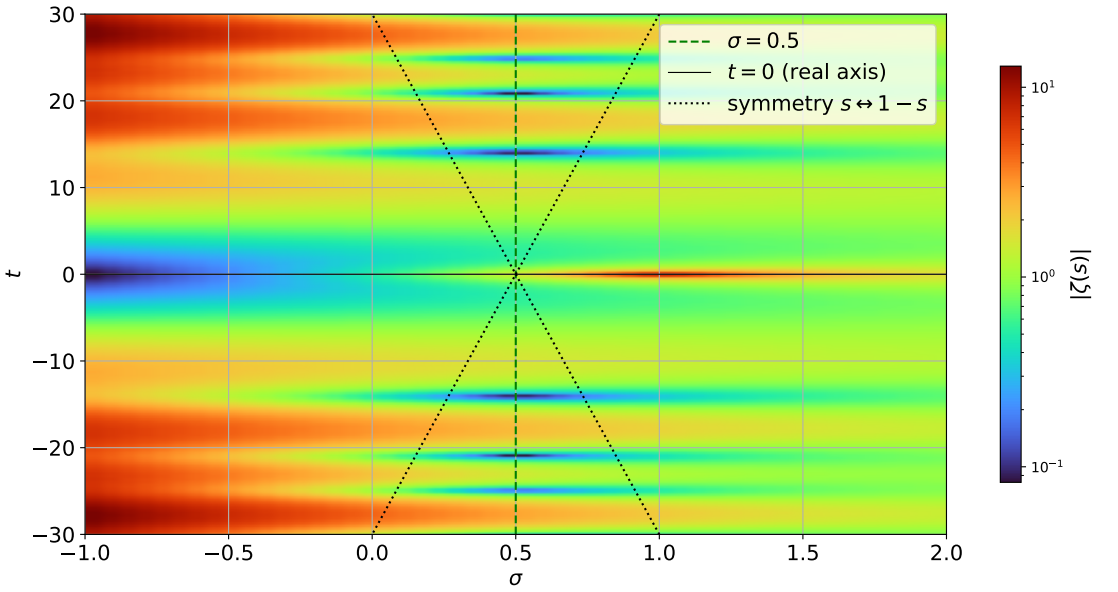

Figure 2: Symmetry of the $|\zeta(s)|$ function in the complex plane

3.3 Interpretation

The difference between the symmetry properties of the two functions suggests a strategy for analyzing the distribution of zeros. If it can be shown that symmetric pairs of zeros may only occur on the line $\sigma = \frac{1}{2}$, this approach provides a natural framework for their localization.

We will show that $|\zeta(s)|$ is asymmetric throughout the critical strip, except on the line $\sigma = \frac{1}{2}$ and for values of s in a restricted domain that we will denote D_R (to be characterized in subsection 5.2.2) In this domain, for well-determined values of s, $|\zeta(s)| \neq 0$, although $|\zeta(s)| = |\zeta(1-s)|$ and $|\chi(s) = 1|$.

Furthermore, since the functions $|\zeta|$ and $|\chi|$, see equations (2) and (6), are symmetric with respect to the σ-axis, it suffices to limit the study to the case $t > 0$. The results can then be extended by symmetry from the positive side to the negative side of the critical strip. The segment $0 < \sigma < 1$ of the real axis and the axes $\sigma = 0$ and $\sigma = 1$, as well as the point $s = 0$, are subject to particular analysis.

3.4 Coupling of $|\zeta(s)|$ Values

From previous observations, we have noted that zeta values work in pairs, $[\zeta(s), \zeta(1-s)]$ or $[\zeta(s), \zeta(\bar{s})]$.

Lemma 1.2 establishes the symmetry of zeros of $\zeta(s)$. This symmetry also applies to the values of $|\zeta(s)|$, hence:

$$\forall s_n \text{ zero of } |\zeta(s)| \text{ in the critical strip } \mathcal{D}^+, \quad |\zeta(s_n)| = 0 \Longleftrightarrow |\zeta(1-s_n)| = 0 \tag{15}$$

This coupling means that zeros of $|\zeta(s)|$ necessarily appear in symmetric pairs: if $|\zeta(s_n)|$ is zero, then $|\zeta(1-s_n)|$ is also zero, and conversely. In the case of moduli the symmetry is with respect to the line $\sigma = \frac{1}{2}$.

Lemma 3.1. *In the critical strip $\mathcal{D}^+$, if $|\chi(s)| = 1$ then $|\zeta(s)| = |\zeta(1-s)|$, in this case, zeros of $|\zeta(s)|$ may potentially exist.*

Proof. From the functional equation $|\zeta(s)| = |\chi(s)| \cdot |\zeta(1-s)|$, equation (5):
If $|\chi(s)| = 1$, then $|\zeta(s)| = |\zeta(1-s)|$.
Two cases arise:

1. If $|\zeta(s)| \neq 0$ then $|\zeta(1-s)| \neq 0$ (situation without zeros)
2. If $|\zeta(s)| = 0$ then $|\zeta(1-s)| = 0$ by equation (15) (situation with zeros)

The condition $|\chi(s)| = 1$ is compatible with the potential existence of zeros.

Lemma 3.2. *In the critical strip $\mathcal{D}^+$, if $|\chi(s)| \neq 1$ then $|\zeta(s)| \neq |\zeta(1-s)|$, and $\zeta(s)$ has no zeros.*

Proof. From the functional equation $|\zeta(s)| = |\chi(s)| \cdot |\zeta(1-s)|$, if $|\chi(s)| \neq 1$ then necessarily $|\zeta(s)| \neq |\zeta(1-s)|$.

Now, if s were a zero of $\zeta(s)$, then by equation (15), we would also have $\zeta(1-s) = 0$, hence $|\zeta(s)| = |\zeta(1-s)| = 0$, which contradicts $|\zeta(s)| \neq |\zeta(1-s)|$. Therefore, if $|\chi(s)| \neq 1$, $\zeta(s)$ cannot have zeros.

4 Study of the $|\chi(s)|$ Function in the Critical Strip $\mathcal{D}^+$

Objective of this section. Now that we have established the crucial role of the $|\chi(s)|$ function in excluding zero-free domains, we will systematically study its behavior in the critical strip. Our goal is to precisely identify the regions where $|\chi(s)| = 1$ and the zeta function may have zeros, and the regions where $|\chi(s)| \neq 1$ in order to eliminate them from the search for zeros.

4.1 Case $\sigma = \frac{1}{2}$, $t > 0$

Let us begin with the simplest case: the critical line $\sigma = \frac{1}{2}$.

According to the relation $\chi(s) \cdot \chi(1-s) = 1$ [3, p. 16, Eq. 2.1.11], for $s = \frac{1}{2} + it$ we have:

$$\begin{aligned} \chi\left(\tfrac{1}{2}+it\right) \cdot \chi\left(1-\left(\tfrac{1}{2}+it\right)\right) &= \chi\left(\tfrac{1}{2}+it\right) \cdot \chi\left(\tfrac{1}{2}-it\right) \\ &= \chi\left(\tfrac{1}{2}+it\right) \cdot \chi\left(\overline{\tfrac{1}{2}+it}\right). \end{aligned}$$

Now, as we showed previously, equation (6), we have $|\chi(s)| = |\chi(\bar{s})|$. We deduce:

$$\left|\chi\left(\tfrac{1}{2}+it\right)\right| \cdot \left|\chi\left(\overline{\tfrac{1}{2}+it}\right)\right| = \left|\chi\left(\tfrac{1}{2}+it\right)\right|^2 = 1.$$

$$\text{Thus,} \quad \left|\chi\left(\tfrac{1}{2}+it\right)\right| = 1 \quad \forall t \in \mathbb{R}. \tag{16}$$

This equality means that on the critical line, the functional equation implies:

$$\left|\zeta\left(\tfrac{1}{2}+it\right)\right| = \left|\zeta\left(1-\left(\tfrac{1}{2}+it\right)\right)\right| = \left|\zeta\left(\overline{1-\left(\tfrac{1}{2}+it\right)}\right)\right|.$$

We observe that the points s and $\overline{1-s}$ are symmetric with respect to the line $\sigma = \frac{1}{2}$. In particular, the points $\frac{1}{2}+it$ and $\overline{1-(\frac{1}{2}+it)}$ coincide, which confirms that on the critical line, the function $|\zeta(s)|$ is symmetric, as are its zeros.

This symmetry relies precisely on the condition $|\chi(s)| = 1$. In accordnace with lemma (3.1), $\zeta(s)$ can potentialy have zeros on this line. Recall that the existence of infinitely many zeros on the critical line $\sigma = \frac{1}{2}$ was demonstrated by Hardy and Littlewood as early as 1914 [3, p. 256, § 10.2], is in accordance with this result.

4.2 Graphical Study of $|\chi(s)|$ Curves in the Critical Strip $\mathcal{D}^+$ for Different $t > 0$ Values

Figure 3 shows the behavior of $|\chi(s)|$ for different values of $t > 0$ in the interval $0 \leq \sigma \leq 1$. We observe that:

- All curves intersect at the critical point $p_c = \left(\frac{1}{2}, 1\right)$, graphically in accordance with equation (16):

$$|\chi\left(\tfrac{1}{2}+it\right)| = 1 \quad \forall t > 0$$

- A special case appears around $t \approx 6.28$ where the curve seems almost constant and equal to 1 over a large part of the critical strip.

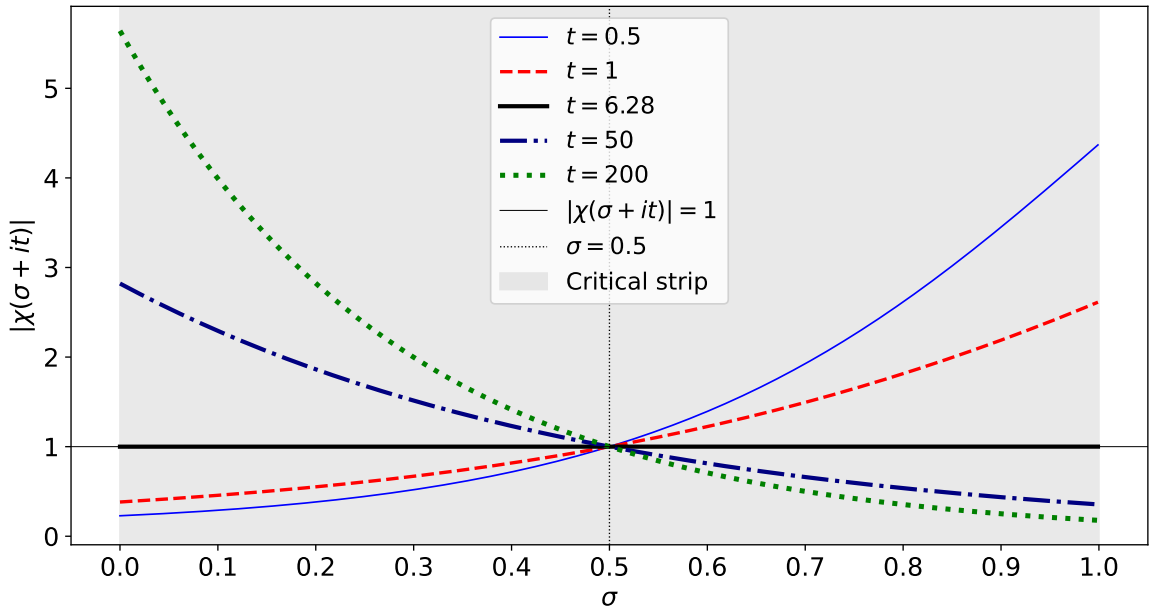

Figure 3: $|\chi(s)|$ for $0 \leq \sigma \leq 1$ and $t \in \{0.5, 1, 6.28, 50, 200\}$

Figure 4 illustrates the dynamic evolution of $|\chi(s)|$ as a function of t, revealing the progressive transition between the different observed regimes.

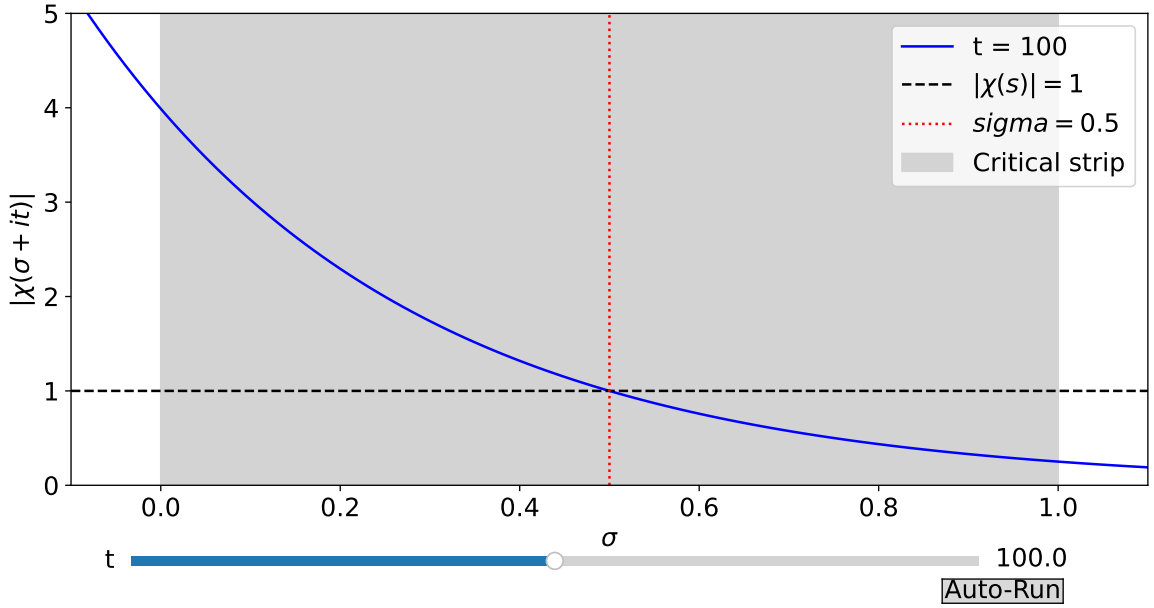

Figure 4: Dynamic evolution of $|\chi(s)|$ as a function of t in the critical strip

In the deposit, we present an interactive Python program using matplotlib that allows real-time visualization of the evolution of $|\chi(s)|$ for $0 \leq \sigma \leq 1$ (see Figure 4).

4.3 Study of the Derivative of $|\chi(s)|$ and Introduction of the Function $g(s) = \frac{1}{|\chi(s)|}\frac{d|\chi(s)|}{d\sigma}$

4.3.1 Logarithmic Derivative of $|\chi(s)|$

To precisely characterize the dynamics of $|\chi(s)|$, we examine the properties of its derivative with respect to σ. Since $|\chi(s)|$ is strictly positive, equation (7), we use its logarithmic derivative.

For a function $f(\sigma, t) \neq 0$, we have:

$$\frac{\partial}{\partial\sigma}\log(f(\sigma,t)) = \frac{\frac{\partial}{\partial\sigma}f(\sigma,t)}{f(\sigma,t)} \Leftrightarrow \frac{\partial}{\partial\sigma}f(\sigma,t) = f(\sigma,t)\cdot\frac{\partial}{\partial\sigma}\log(f(\sigma,t)) \tag{17}$$

Let $s = \sigma + it$, with σ variable and $t > 0$ a parameter. This approach allows us to differentiate with respect to σ while considering t as constant. We then have:

$$\frac{d}{d\sigma}\log(f(s)) = \frac{d}{ds}\log(f(s))\cdot\frac{ds}{d\sigma}$$

Since $s = \sigma + it$, we have $\dfrac{ds}{d\sigma} = 1$, hence:

$$\frac{d}{d\sigma}\log\left(f(s)\right) = \frac{d}{ds}\log\left(f(s)\right) \tag{18}$$

Recall that if $f(s) \neq 0$:

$$f(s) = |f(s)|\cdot e^{i\arg(f(s))} \Leftrightarrow \log f(s) = \log|f(s)| + i\arg(f(s))$$

hence:

$$\log|f(s)| = \Re(\log f(s)) \tag{19}$$

Combining these results, we finally obtain:

$$\frac{d}{d\sigma}|\chi(s)| = |\chi(s)| \cdot \frac{d}{d\sigma}\log|\chi(s)| = |\chi(s)| \cdot \frac{d}{ds}\Re(\log\chi(s)) \tag{20}$$

Given that $|\chi(s)| > 0 \ \forall t$, see equation (7), we will focus only on the factor $\frac{d}{d\sigma}\log|\chi(s)|$ of the derivative, since it is this term that determines zero crossings and sign changes.

4.3.2 Expression of the Derivative $\frac{d}{d\sigma}\log|\chi(s)|$

Developing $\log\chi(s)$ from equation (4):

$$\begin{aligned}
\frac{d}{ds}\log|\chi(s)| &= \frac{d}{ds}\Re\left[\log\left(\pi^{s-\frac{1}{2}} \cdot \frac{\Gamma\left(\frac{1-s}{2}\right)}{\Gamma\left(\frac{s}{2}\right)}\right)\right] \\
&= \frac{d}{ds}\Re\left[\log\pi^{s-\frac{1}{2}} + \log\Gamma\left(\tfrac{1-s}{2}\right) - \log\Gamma\left(\tfrac{s}{2}\right)\right] \\
&= \Re\left[\frac{d}{ds}\log\pi^{s-\frac{1}{2}}\right] + \Re\left[\frac{d}{ds}\log\Gamma\left(\tfrac{1-s}{2}\right)\right] - \Re\left[\frac{d}{ds}\log\Gamma\left(\tfrac{s}{2}\right)\right]
\end{aligned}$$

Introducing the digamma function $\psi(s) = \frac{d}{ds}\log\Gamma(s)$ [4, p. 58, Sec 6.3], we obtain:

$$\frac{d}{ds}\log|\chi(s)| = \log\pi - \tfrac{1}{2}\left(\Re\left[\psi\left(\tfrac{1-s}{2}\right)\right] + \Re\left[\psi\left(\tfrac{s}{2}\right)\right]\right) \tag{21}$$

4.3.3 Definition of the Function $\mathrm{g}(s)$

We define the function:

$$\mathrm{g}(s) = \frac{1}{|\chi(s)|}\frac{d|\chi(s)|}{d\sigma} = \log\pi - \tfrac{1}{2}\left(\Re\left[\psi\left(\tfrac{1-s}{2}\right)\right] + \Re\left[\psi\left(\tfrac{s}{2}\right)\right]\right) \tag{22}$$

4.3.4 Properties of $\mathrm{g}(s)$

- **Symmetry**: $g(1-s) = \mathrm{g}(s)$ (symmetry with respect to $\sigma = \frac{1}{2}$)
- **Constant term**: $\log\pi \approx 1.14472989$ (positive)
- **Variable term**: $-\frac{1}{2}\left(\Re\left[\psi\left(\frac{1-s}{2}\right)\right] + \Re\left[\psi\left(\frac{s}{2}\right)\right]\right)$ (can be positive or negative depending on t and σ)

The function $\mathrm{g}(s)$ will determine the variations of $|\chi(s)|$ and notably its monotonicity.

4.4 Study of the Function $\mathrm{g}(s)$ in the Critical Strip near $t = 6.28$

4.4.1 Graphical Analyses and Observations

The graphical analysis of $\mathrm{g}(s)$ (Figure 5) reveals that:

- The function is symmetric with respect to the axis $\sigma = \frac{1}{2}$
- The curve presents an extremum at $\sigma = \frac{1}{2}$ for all t
- Near $t = 6.28$, the function changes sign
- For sufficiently large t, the curve becomes concave

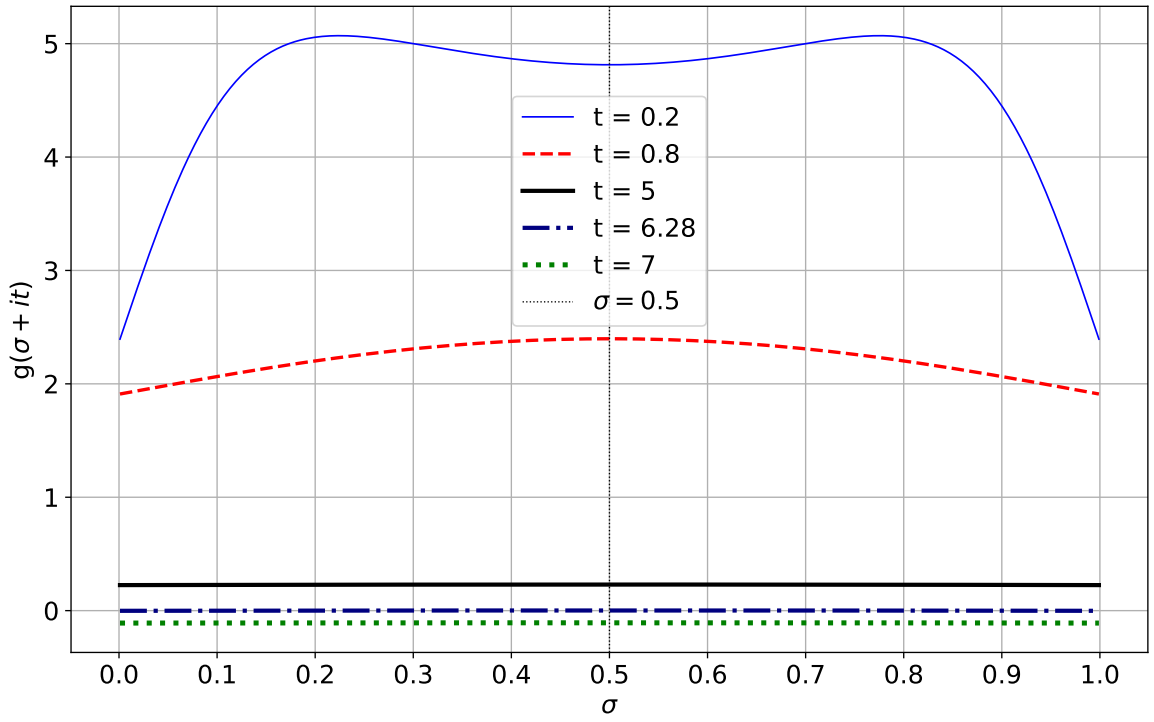

Figure 5: $\mathrm{g}(s)$ for $s = \sigma + it$, $0 \leq \sigma \leq 1$, $t \in \{0.2, 0.8, 5, 6.28, 7\}$

4.4.2 Proof of $\mathrm{g}(s)$ of the Extremum at $\sigma = \frac{1}{2}$

We first compute the derivative of $g(s)$ with respect to σ. From the definition of $g(s)$ in (22):

$$g'(s) = \frac{\partial}{\partial \sigma} g(\sigma + it) = -\frac{1}{4}\left[\Re\left(\psi'\left(\frac{s}{2}\right)\right) - \Re\left(\psi'\left(\frac{1-s}{2}\right)\right)\right] \tag{23}$$

where ψ' denotes the trigamma function.
Now, evaluating this derivative at $\sigma = \frac{1}{2}$, i.e., at $s = \frac{1}{2} + it$, we obtain:

$$g'\left(\tfrac{1}{2} + it\right) = -\frac{1}{4}\left[\Re\psi'\left(\tfrac{1}{4} + \tfrac{it}{2}\right) - \Re\psi'\left(\tfrac{1}{4} - \tfrac{it}{2}\right)\right] \tag{24}$$

Using the property $\psi'(\overline{z}) = \overline{\psi'(z)}$, we have:

$$\psi'\left(\tfrac{1}{4} + \tfrac{it}{2}\right) = \overline{\psi'\left(\tfrac{1}{4} - \tfrac{it}{2}\right)}$$

and consequently:

$$\Re\left(\psi'\left(\tfrac{1}{4} + \tfrac{it}{2}\right)\right) = \Re\left(\psi'\left(\tfrac{1}{4} - \tfrac{it}{2}\right)\right)$$

Therefore:

$$g'\left(\tfrac{1}{2} + it\right) = 0 \quad \forall t \in \mathbb{R} \tag{25}$$

This shows that $\sigma = \frac{1}{2}$ is a critical point of $g(s)$ for all t.

4.5 Study of the Concavity of $\mathrm{g}(s)$

4.5.1 $\mathrm{g}''(s)$Graphical observations

To determine the concavity of $\mathrm{g}(s)$, we must study the sign of the second derivative of the function $\mathrm{g}(s)$. This function is given by:

$$g''(s) = -\frac{1}{8}\left(\Re\left[\psi''\left(\frac{1-s}{2}\right)\right] + \Re\left[\psi''\left(\frac{s}{2}\right)\right]\right) \tag{26}$$

ψ'' represents the polygamma function of order 2. Figure 6 shows the evolution of $g''(s)$ for different values of t. We observe the symmetry with respect to $\sigma = \frac{1}{2}$ and the systematic presence of an extremum at this point for $\sigma = \frac{1}{2}$ $\forall t$.The Figure 6 bis represents a zoom of the upper left corner of Figure 6.

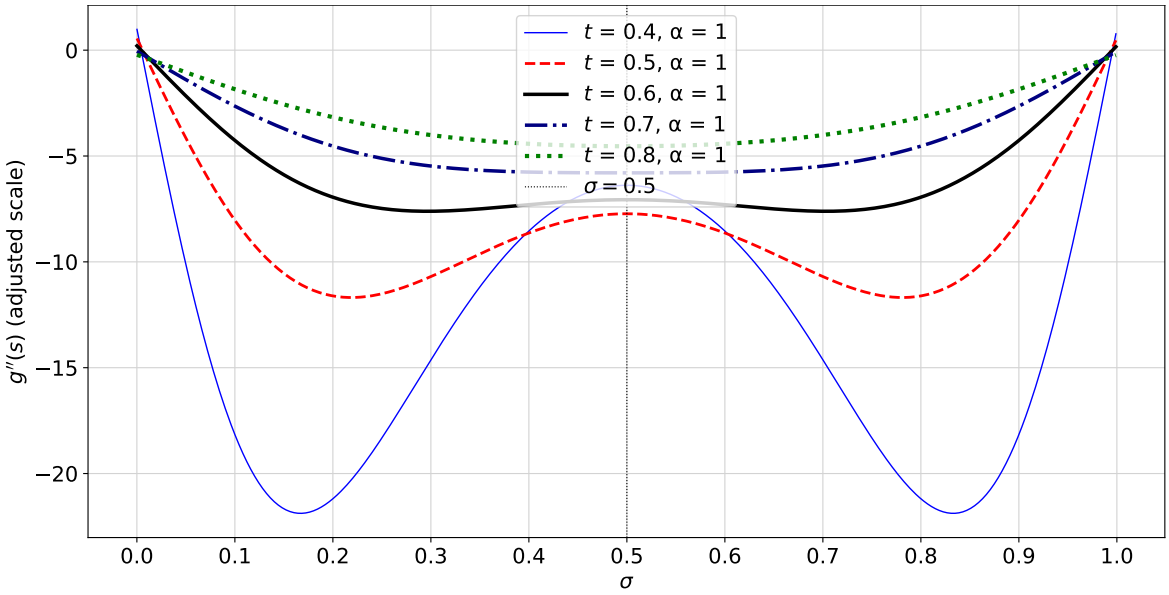

Figure 6: Evolution of $g''(s)$ for $t \in \{0.4, 0.5, 0.6, 0.7, 0.8\}$ (without scale correction α)

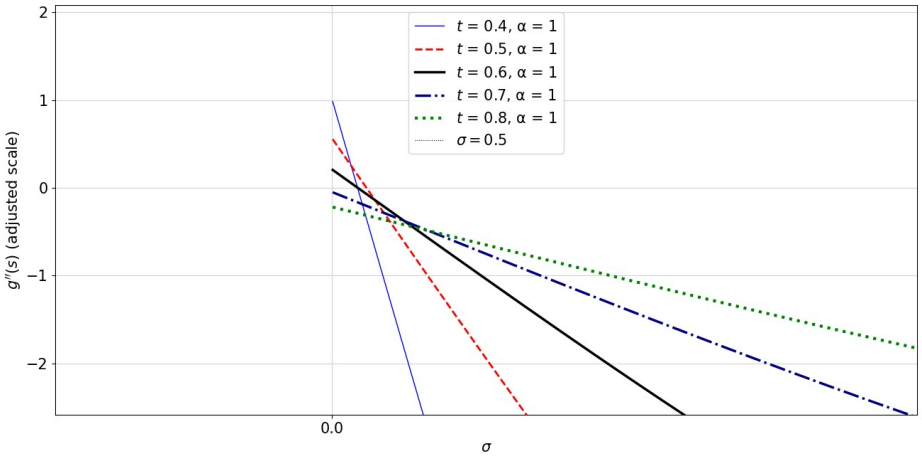

Figure 6 bis - Enlargement of Figure 6 at $\sigma = 0$ in the neighborhood of $0.4 \leq t \leq 0.8$

4.5.2 Critical Point of Negativity of $g''(s)$

After preliminary graphical research, we found that $g''(s)$ can become negative for $0.6 < t < 0.7$, see Figures 6 and 6 bis. (The multiplicative coefficient α was used during the preliminary research phase to observe the shape of the curves for different values of t). Indeed, for $0.6 < t < 0.7$, $g''(s)$ is almost convex and $g''(0,t)$ corresponds to the maximum of the curve. The entirety of $g''(s)$ is bounded by two parallel horizontal lines drawn from the points $g''(0,t)$ and $g''(0.5,t)$. The analysis of the curves $g''(0,t)$ and $g''(0.5,t)$, Figure 7, reveals that $g''(s)$ becomes strictly negative for $t > t_0 \approx 0.678157$. t_0 is the solution of the equation:

$$g''(0 + it) = 0$$

This value was determined numerically by the brentq method implemented in Python in the interval [0.6,0.7]. The value $t_0 \approx 0.678156835255537$ corresponds to the point where $g''(0+it)$ vanishes, marking the transition to strict concavity of $g(s)$ for $t > t_0$.

4.5.3 Certified Critical Point t_0 of $g''(0 + it)$

To rigorously determine the transition to strict concavity, we evaluate $g''(0 + it)$ over the interval $t \in [0.6, 0.7]$ using **Arb interval arithmetic**.

- $g''(0 + 0.6\,i) \approx 0.208853665084718 > 0$
- $g''(0 + 0.7\,i) \approx -0.048104767104586 < 0$

This ensures the existence of a unique root t_0 in $[0.6, 0.7]$ such that

$$g''(0 + it_0) = 0.$$

Using rigorous bisection with Arb, we obtain

$$t_0 \approx 0.678156835255537.$$

This certified value of t_0 will be used as the lower bound in subsequent concavity verifications of $g(s)$ for $t > t_0$.

4.5.4 Asymptotic Behavior

For $s = it$ with $t \gg 1$, using the asymptotic expansion [4, p. 260, Eq 6.4.13]:

$$\psi''(z) \sim -\frac{1}{z^2} - \frac{1}{z^3} - \frac{1}{2z^4} - \cdots, \quad |z| \to \infty$$

we obtain:

$$g''(it) \sim -\frac{1}{t^2} + O\left(\frac{1}{t^4}\right)$$

This confirms that $g''(s)$ remains negative for large values of t.

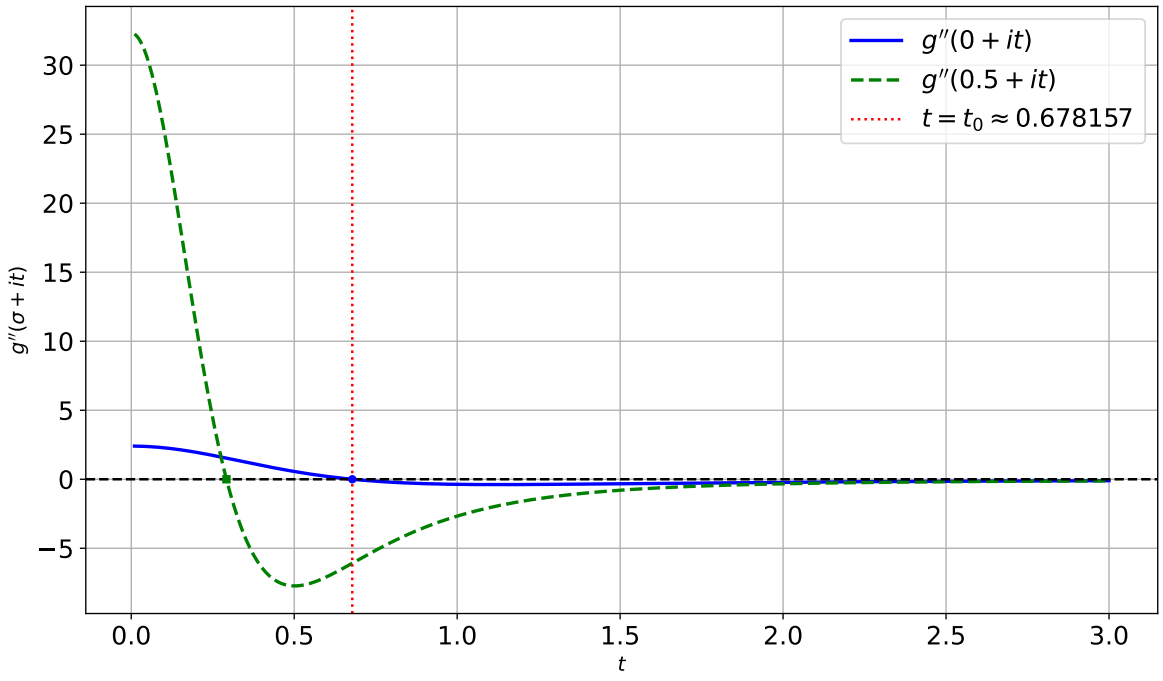

Figure 7: Critical point t_0 from which $g''(s)$ becomes strictly negative

This established concavity of g(s) for $t \geq t_0$ and will allow us to rigorously determine its sign in the vicinity of $t = 6.28$.

4.5.5 Proof of the Strict Concavity of $g(s)$ for $\sigma \in [0, 1]$ $t > t_0$

A. Series Representation of the Second Derivative.

The second derivative $g''(\sigma, t)$ of the function $g(s)$ can be expressed using the partial fraction expansion of the tetragamma function:

$\psi^{(2)}(z) = -2\sum_{n=0}^{\infty}(n+z)^{-3}$.[4, p. 260, Eq 6.4.10].

For $s = \sigma + it$ and $\sigma \in (0, 1)$, we have:

$$g''(\sigma, t) = \frac{1}{4}\sum_{n=0}^{\infty}\left[f(x_n, y) + f(x'_n, y)\right], \tag{27}$$

where the variables are defined as:

- $y = t/2$ (the scaled imaginary component).
- $x_n = n + \frac{\sigma}{2}$ and $x'_n = n + \frac{1-\sigma}{2}$ (the real parts of the poles).
- The kernel function $f(x, y) = \text{Re}\left(\frac{1}{(x+iy)^3}\right) = \frac{x(x^2-3y^2)}{(x^2+y^2)^3}$.

B. Sign Analysis of the Kernel Function.

The sign of each individual term in the series is determined solely by the numerator of the kernel $f(x, y)$. Since $x > 0$ for all $n \geq 0$ and $\sigma \in (0, 1)$, we observe:

$$f(x, y) < 0 \iff x^2 - 3y^2 < 0 \iff x < y\sqrt{3}.$$

At the threshold $t_0 \approx 0.678157$, the scaled variable is $y \approx 0.339078$, yielding a critical value:

$$x_{crit} = y\sqrt{3} \approx 0.339078 \times 1.732 \approx 0.5873.$$

C. Rigorous Justification of the $n = 0$ Term Dominance.

We first consider $\sigma \in (0, 0.5)$. For such σ, the real parts of the first term ($n = 0$) are bounded by $\max(x_0, x'_0) = 0.5$, where $x_0 = \frac{1-\sigma}{2}$ and $x'_0 = \frac{\sigma}{2}$. Since $0.5 < 0.5873$, this ensures that $f(x_0, y) < 0$ and $f(x'_0, y) < 0$ for all $t \geq t_0$.

The case $\sigma \in (0.5, 1)$ follows by symmetry of g$''(s)$ with respect to the ctritical line $\sigma = 0.5$. Indeed, the second derivative satisfies $g''(\sigma, t) = g''(1 - \sigma, -t)$, so the negativity established on $(0, 0.5)$ extends directly to $(0.5, 1)$. Therefore, it suffices to prove that the negative component dominates the sum on $(0, 0.5)$. the result for the full interval[0,1] the result for the full interval $[0, 1]$ is then obtained by symmetry and continuity of $g''(s)$.

To complete the proof, we now establish the following bounds that guarantee the dominance of the negative $n = 0$ term over the remaining series:

1. **Lower Bound for the Negative Component (S_0):** The term $S_0(\sigma, t) = f(x_0, y) + f(x'_0, y)$ reaches its least negative value at the midpoint $\sigma = 0.5$ ($x_0 = x'_0 = 0.25$). At t_0, we calculate:

$$S_0(\sigma, t) \leq 2 \cdot f(0.25, 0.339) \approx -25.30.$$

2. **Upper Bound for the Positive Remainder (R):** For $n \geq 1$, we use the majorant $f(x, y) < x^{-3}$. The positive remainder $R = \sum_{n=1}^{\infty}[f(x_n, y) + f(x'_n, y)]$ is maximized as $\sigma \to 0$:

$$R(\sigma, t) < \sum_{n=1}^{\infty} n^{-3} + \sum_{n=1}^{\infty}(n + 0.5)^{-3} = \zeta(3) + [7\zeta(3) - 8] \approx 1.202 + 0.414 = 1.616,$$

where $\zeta(3) \approx 1.202$ is Apéry's constant and $\zeta(3, 0.5) = 7\zeta(3)$ is a property of the Hurwitz zeta function.

The magnitude of the negative term S_0 is more than 14 times larger than the maximum positive contribution of the remainder R, as $|-25.30| \gg 1.616$. This gap rigorously ensures that $g''(\sigma, t) < 0$ across the entire interval.

D. Temporal Extension

for $t > t_0$ As t increases beyond t_0, the scaled variable y increases. This expansion of the "negative zone" ($x < y\sqrt{3}$) further decreases the values of the dominant terms $f(x_0, y)$ and $f(x'_0, y)$, while shifting more terms of the remainder R from positive to negative. Consequently, the second derivative $g''(\sigma, t)$ remains strictly negative for all $t > t_0$.

Conclusion For all $t > t_0$ and all $\sigma \in [0, 1]$, the dominant negative terms of the tetragamma expansion ensure that $g''(\sigma, t) < 0$. Thus, the function $g(s)$ is **strictly concave** with respect to σ on the interval $[0, 1]$ for any t exceeding the threshold t_0 and will allow us to rigorously determine its sign in the vicinity of $t = 6.28$.

4.6 Analytic Study of g(s) in $\mathcal{D}^+$.

4.6.1 Proof of the Positivity of $g(s)$ on $0 \leq \sigma \leq 1,\ 0 < t \leq t_0 = 0.678157$

Given the symmetry of the function g(s) with respect to the critical line $\sigma = 0.5$, the proof is carried out on $0 < \sigma < 0.5$.

1) Introduction and Notation Let $s = \sigma + it$. We define the real variables

$$x_1 = \frac{\sigma}{2}, \quad x_2 = \frac{1 - \sigma}{2}, \quad y = \frac{t}{2} \in (0, 0.3391].$$

We study

$$S(\sigma, t) = \Re\psi(x_1 + iy) + \Re\psi(x_2 + iy).$$

Using the Weierstrass series representation for $\Re(z) > 0$ of the digamma function, [4, p. 259, Eq 6.3.16]:

$$\Re\psi(x + iy) = -\gamma + T_0(x, y) + \sum_{n=1}^{\infty} T_n(x, y) \tag{28}$$

Where γ is the constant of Euler-Mascheroni and

$$T_0(x, y) = 1 - \frac{x}{x^2 + y^2}, \quad T_n(x, y) = \frac{1}{n + 1} - \frac{n + x}{(n + x)^2 + y^2}.$$

To justify the upper bound of the series tail, we rearrange $T_n(x, y)$ over a common denominator:

$$T_n(x, y) = \frac{n(x - 1) + x(x - 1) + y^2}{(n + 1)((n + x)^2 + y^2)}. \tag{29}$$

Given that $x \leq 0.5$, the quantity $(x - 1)$ is negative, implying $n(x - 1) + x(x - 1) \leq 0$ for all $n \geq 1$. Consequently, the numerator is bounded by y^2. Since the denominator satisfies $(n + 1)((n + x)^2 + y^2) > n^3$ for $x, y^2 > 0$, we obtain the following majorization:

$$\sum_{n=1}^{\infty} T_n(x, y) \leq \sum_{n=1}^{\infty} \frac{y^2}{n^3} = y^2\zeta(3) \leq 0.1382, \tag{30}$$

where the numerical constant follows from $\zeta(3) \approx 1.202$ and the specific range of y under consideration.

2) Phase 1: Behavior at the Boundary $\sigma \to 0^+$ It is crucial to examine the limit of $S(\sigma, t)$ as $\sigma \to 0^+$ for fixed t (thus fixed y):

$$\lim_{x_1 \to 0^+} T_0(x_1, y) = 1 - \frac{0}{0^2 + y^2} = 1.$$

At this limit, $x_2 \to 0.5$. The sum of the principal terms is
$F_0 = T_0(x_1, y) + T_0(x_2, y) \quad \longrightarrow \quad L(y) = 2 - \frac{0.5}{0.25+y^2}$ as $\sigma \to 0^+$ $(x_1 \to 0, x_2 \to 0.5)$

This function increases with y. At $y_{\max} = 0.3391$:

$$L(0.3391) \approx 2 - \frac{0.5}{0.25 + 0.115} \approx 0.6301.$$

Including the series tail contribution, we have

$$S_{\lim} \leq -2\gamma + 0.6301 + 2 \cdot 0.1382 \approx -0.2479 < 0.$$

Hence,

$$g(s) \geq \log \pi + 0.1239 \approx 1.2686 > 0$$

near $\sigma = 0$.

3) Phase 2: Interior Interval $0.01 \leq \sigma \leq 0.5$ On this compact interval, $x_1 \in [0.005, 0.25]$ and $x_2 \in [0.25, 0.495]$. The principal term

$$F_0 = T_0(x_1, y) + T_0(x_2, y)$$

is maximal at the left boundary of the interval. Evaluating at $y = 0.3391$:

- $\sigma = 0.01$ $(x_1 = 0.005)$: $F_0 \approx 0.9565 - 0.3749 = 0.5816$,
- $\sigma = 0.5$ $(x_1 = 0.25)$: $F_0 = 2 \cdot (-0.4085) = -0.8170$.

The maximum of F_0 on this interval is below the limit value 0.6301 found in Phase 1. Adding the series tail, we get

$$S(\sigma, t) \leq -2\gamma + 0.5816 + 0.2764 \approx -0.2960 < 0.$$

Thus,

$$g(s) = \log \pi - \frac{1}{2} S(\sigma, t) \geq \log \pi + 0.1480 \approx 1.293 > 0.$$

4) General Conclusion Combining Phase 1 and Phase 2, the sum of real parts $S(\sigma, t)$ is strictly negative throughout the domain $\sigma \in (0, 0.5]$. Consequently,

$$g(s) > 0 \quad \text{for } \leq \sigma \leq 1,\ 0 < t \leq 0.678157$$

4.6.2 Proof that $\frac{\partial}{\partial t} g(\sigma + it) < 0$ for $\sigma \in [0, 1]$ and $t > 0$

Define

$$g(s) = \log \pi - \frac{1}{2} \operatorname{Re}\left[\psi\left(\frac{1 - s}{2}\right) + \psi\left(\frac{s}{2}\right)\right], \qquad s = \sigma + it,$$

where ψ is the digamma function.

1) Rewriting :
Set

$$z_1 = \frac{1-\sigma-it}{2}, \qquad z_2 = \frac{\sigma+it}{2},$$

and

$$h(\sigma,t) = \operatorname{Re}\big[\psi(z_1)+\psi(z_2)\big].$$

Then $g(\sigma+it) = \log\pi - \frac{1}{2}h(\sigma,t)$, so

$$\frac{\partial g}{\partial t} = -\frac{1}{2}\frac{\partial h}{\partial t}.$$

2) Computing $\partial h/\partial t$:

$$\frac{\partial h}{\partial t} = \operatorname{Re}\left[-\frac{i}{2}\psi'(z_1) + \frac{i}{2}\psi'(z_2)\right] = \frac{1}{2}\operatorname{Im}\psi'(z_1) - \frac{1}{2}\operatorname{Im}\psi'(z_2).$$

3) Sign of $\operatorname{Im}\psi'(x+iy)$:
For $y \neq 0$,[4, p. 260, Eq 6.4.10].

$$\psi'(x+iy) = \sum_{n=0}^{\infty} \frac{1}{(n+x+iy)^2}$$

gives

$$\operatorname{Im}\psi'(x+iy) = -2\sum_{n=0}^{\infty} \frac{(n+x)\,y}{\big((n+x)^2+y^2\big)^2}.$$

Since $n+x>0$ for all $n \geq 0$, each term in positf and the series converges to a positive value.It follows that:

$$\operatorname{sign}\big(\operatorname{Im}\psi'(x+iy)\big) = -\operatorname{sign}(y).$$

4) Applying to z_1 **and** z_2 For $t>0$,

$$z_1 = \frac{1-\sigma}{2} - i\frac{t}{2} \implies y_1 = -\frac{t}{2} < 0 \implies \operatorname{Im}\psi'(z_1) > 0,$$

$$z_2 = \frac{\sigma}{2} + i\frac{t}{2} \implies y_2 = +\frac{t}{2} > 0 \implies \operatorname{Im}\psi'(z_2) < 0.$$

These signs are independent of σ.

5) Conclusion

$$\frac{\partial h}{\partial t} = \underbrace{\frac{1}{2}\operatorname{Im}\psi'(z_1)}_{>0} - \underbrace{\frac{1}{2}\operatorname{Im}\psi'(z_2)}_{<0} > 0.$$

Hence

$$\frac{\partial g}{\partial t} = -\frac{1}{2}\frac{\partial h}{\partial t} < 0 \qquad \text{for } 0 \leq \sigma \leq 1 \text{ and } t>0.$$

4.6.3 Proof of $g(s)<0$ for $t>t_3$ and $\sigma \in [0,1]$

We have :

1) **Decay in** t**:** $\dfrac{\partial g}{\partial t}(s) < 0$ for all $\sigma \in (0,1)$, $t>0$.

2) **Concavity in** σ**:** $\dfrac{\partial^2 g}{\partial \sigma^2}(s) < 0$ for all $\sigma \in [0,1]$, $t>t_3$.

3) **Symmetry:** $g(\sigma,t) = g(1-\sigma,-t)$, hence $\dfrac{\partial g}{\partial \sigma}(\frac{1}{2},t) = 0$.

By definition, t_3 satisfies $g(\frac{1}{2}+it_3) = 0$. From 1), for any $t > t_3$:

$$g(\tfrac{1}{2}+it) < g(\tfrac{1}{2}+it_3) = 0.$$

Properties 2) and 3) imply that for fixed $t > t_3$, the function $\sigma \mapsto g(\sigma+it)$ attains its maximum at $\sigma = \frac{1}{2}$. Therefore, for all $\sigma \in [0,1]$:

$$g(\sigma+it) \le g(\tfrac{1}{2}+it) < 0.$$

Thus $g(s) < 0$ for every $\sigma \in [0,1]$ and $t > t_3$.

4.6.4 Asymptotic Analysis of $g(s)$ for $t \gg 1$ and any $\sigma \in [0,1]$

Method: Asymptotic expansion of the digamma function $\psi(z)$.

Steps:

- **Expansion of ψ:** For $|z| \to \infty$, [4, p. 259, Eq 6.3.18]:

$$\psi(z) = \log z - \frac{1}{2z} - \frac{1}{12z^2} + O\left(\frac{1}{z^4}\right).$$

- **Application** to $z_1 = \frac{1-s}{2}$ and $z_2 = \frac{s}{2}$ with $s = \sigma + it$.
- **Calculation** of the real part of $\psi(z_1) + \psi(z_2)$:

$$\mathrm{Re}[\psi(z_1)+\psi(z_2)] = 2\log\left(\frac{t}{2}\right) + \frac{1}{t^2} + O\left(\frac{1}{t^3}\right).$$

- **Expression** of $g(\sigma,t)$:

$$g(\sigma,t) = \log\left(\frac{2\pi}{t}\right) + O\left(\frac{1}{t^2}\right).$$

- **Sign:** For $t > 2\pi \approx 6.28$, $\log(2\pi/t) < 0$. The correction term is negligible for $t \gg 1$.

Conclusion: For sufficiently large t, $g(\sigma,t) < 0$ for every $\sigma \in [0,1]$. This confirms and reinforces our previous result.

4.7 Characterization of $|\chi(s)|$ near $t = 6.28$. Critical Values t_1, t_2, t_3

4.7.1 Analytical Foundations

Before proceeding to the detailed analysis of the behavior of $|\chi(s)|$ in the vicinity of $t = 6.28$, we recall the fundamental analytical properties that will be employed throughout this section. These properties have been established rigorously in the preceding sections and constitute the theoretical backbone of our investigation.

- **Symmetry of $g(s)$ with respect to $\sigma = \frac{1}{2}$,** (see subsection 4.3.4):

$$g(\sigma+it) = g(1-\sigma-it), \quad \forall \sigma \in [0,1],\ t > 0.$$

- **Concavity of $g(s)$ for $t > t_0$,** (see subsection 4.5.5):

$$\frac{\partial^2 g}{\partial \sigma^2}(s) < 0 \quad \text{for } t > t_0,\ \sigma \in [0,1].$$

The concavity in σ implies that for fixed $t > t_0$, the function g attains its maximum at $\sigma = \frac{1}{2}$ and its minimum at $\sigma = 0$ and $\sigma = 1$, while being strictly increasing on $[0, \frac{1}{2}]$ and strictly decreasing on $[\frac{1}{2}, 1]$.

- **Positivity of $g(s)$ for $t < t_0$**, (see subsection 4.6.1):

$$g(s) > 0 \quad \text{for all } \sigma \in [0,1],\ 0 < t < t_0 \approx 0.678157.$$

  This property ensures the monotonic behavior of $|\chi(s)|$ in the low t regime.

- **Negativity of the t-derivative of $g(s)$**, (see subsection 4.6.2):

$$\frac{\partial g}{\partial t}(s) < 0 \quad \text{for all } \sigma \in (0,1),\ t > 0.$$

  This monotonicity in t guarantees the uniqueness of the critical values t_1, t_2, and t_3 defined respectively by the equations $g(0+it) = 0$, $|\chi(0+it)| = 1$, and $g(\frac{1}{2}+it) = 0$.

- **Analytical proof of $g(s) < 0$ for $t > t_3$ and every $\sigma \in [0,1]$**, (see subsection 4.6.3):
  This property ensures the $|\chi(s)|$ strictly decreasing for $t > t_3$ and every $\sigma \in [0,1]$.

These five properties provide a complete analytical framework for understanding the evolution of $|\chi(s)|$ as t increases through the critical region near $t = 6.28$. In particular, they allow us to determine precisely the number of intersections of the curve $\sigma \mapsto |\chi(\sigma + it)|$ with the horizontal line $y = 1$.

4.7.2 Simultaneous behavior of $g(s)$ and $|\chi(s)|$ for different values of t in the critical strip

Using an interactive Python program (provided in our deposit), we analyzed the simultaneous behavior of $g(s)$ and $|\chi(s)|$ for different values of t in the critical strip $\mathcal{D}^+$ near $t = 6.28$. Figures 8 to 12 illustrate this study.

We identified three critical values of t that characterize the evolution of $g(s)$ and $|\chi(s)|$ simultaneously. These values delineate the domains where $|\chi(s)| = 1$ and where $|\chi(s)| \neq 1$:

- $t_1 \approx 6.269845775920849$
- $t_2 \approx 6.283185340798241$
- $t_3 \approx 6.289835988836902$

A. $0 < t < t_1 \approx 6.26985$ **(Figure 8)**

This regime is decomposed into two phases: $t \in (0, t_0]$ and $t \in (t_0, t_1]$.

- For $t \in (0, t_0]$, $g(s) > 0$ for all $\sigma \in [0,1]$; its global minimum is positive (see subsection 4.6.1).
- For $t \in (t_0, t_1]$, $g(s) > 0$ for all $\sigma \in [0,1]$; its global minimum remains positive due to the concavity of $g(s)$ and the fact that $g(0,t) > 0$ for $t < t_1$.
- Consequently, $|\chi(s)|$ is strictly increasing in σ.
- $|\chi(s)|$ intersects the line $|\chi(s)| = 1$ only at $\sigma = \frac{1}{2}$.
- On the critical axis $\sigma = \frac{1}{2}$, $|\zeta(s)|$ may potentially vanish.

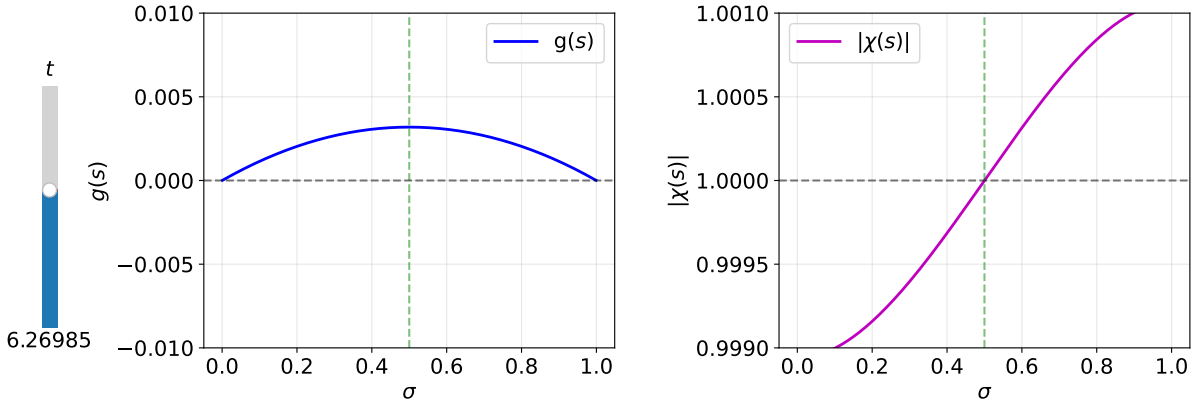

Figure 8: $g(s) > 0$ for $t < 6.26985$. $|\chi(s)|$ intersects $|\chi(s)| = 1$ only at $(\frac{1}{2}, 1)$.

B. Intermediate Case: t between t_1 and t_2 ($t = 6.27557$) (Figure 9)

- The sign of $g(s)$ varies with σ.
- $g(s)$ vanishes at two points symmetric with respect to $\sigma = \frac{1}{2}$.
- $|\chi(s)|$ is non-monotonic and intersects the line $|\chi(s)| = 1$ at a single point $(\frac{1}{2}, 1)$.
- On the critical axis $\sigma = \frac{1}{2}$, $|\chi(\frac{1}{2}, t)| = 1$, and $|\zeta(s)|$ may potentially vanish.

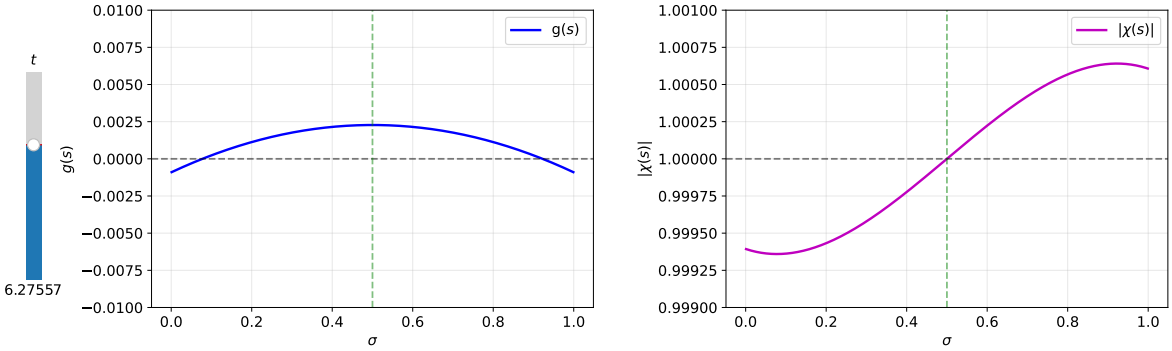

Figure 9: For $t = 6.27557$, the sign of $g(s)$ varies with σ. $|\chi(s)|$ is non-monotonic and intersects the line $|\chi(s)| = 1$ at a single point $(\frac{1}{2}, 1)$.

C. Regime 2: $t_2 \leq t < t_3$

Case $t = t_2 \approx 6.28318$ (Figure 10)

- The sign of $g(s)$ varies with σ.
- $g(s)$ vanishes at two points symmetric with respect to $\sigma = \frac{1}{2}$.
- $|\chi(s)|$ is non-monotonic and passes through three intersection points centered at $(\frac{1}{2}, 1)$.
- $|\zeta(s)| = |\zeta(1 - s)|$ for three values of σ centered on $\sigma = \frac{1}{2}$, giving three possibilities for $|\zeta(s)| = 0$.
- If t decreases, we return to a situation similar to the previous intermediate case (Figure 9), where $|\chi(s)|$ is non-monotonic and intersects at a single point $(\frac{1}{2}, 1)$.

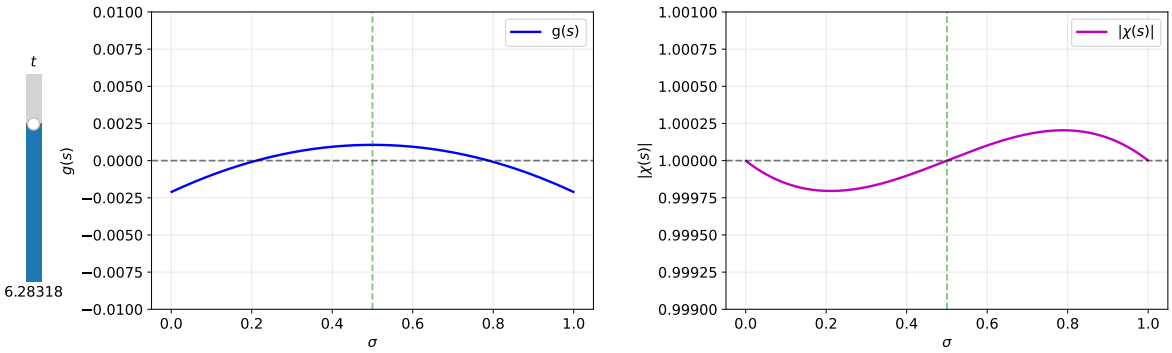

Figure 10: For $t = t_2 \approx 6.28318$, the sign of $g(s)$ varies with σ. The curve $|\chi(s)|$ intersects the line $|\chi(s)| = 1$ at a single point $(\frac{1}{2}, 1)$ and passes through three points as t increases.

D. Intermediate Case: t between t_2 and t_3 ($t = 6.28512$) (Figure 11)

- The sign of $g(s)$ varies with σ.
- $g(s)$ vanishes at two points symmetric with respect to $\sigma = \frac{1}{2}$.
- $|\chi(s)|$ is non-monotonic and passes through three intersection points centered at $(\frac{1}{2}, 1)$.
- $|\zeta(s)| = |\zeta(1-s)|$ for three values of σ centered on $\sigma = \frac{1}{2}$, giving three possibilities for $|\zeta(s)| = 0$.

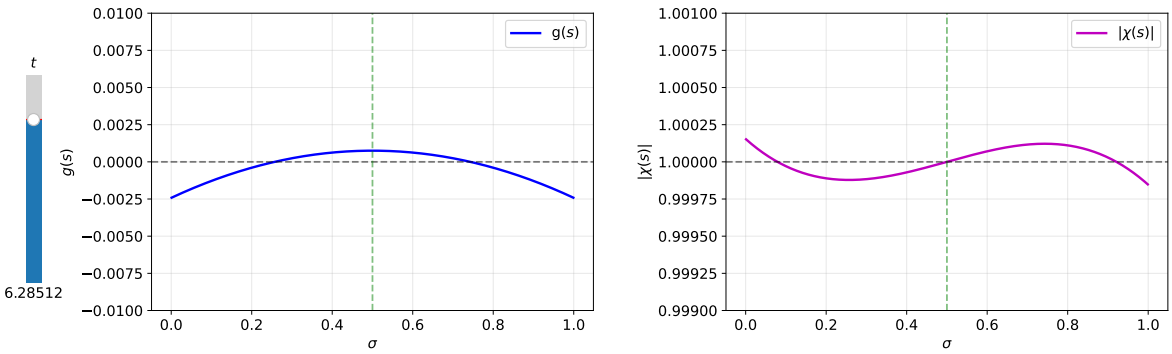

Figure 11: For $t = 6.28512$, the sign of $g(s)$ varies with σ. $|\chi(s)|$ is non-monotonic and passes through three points on the line $|\chi(s)| = 1$.

E. Regime 3: $t \geq t_3 \approx 6.28983$ (Figure 12)

- The study of $g(s)$ for $\sigma \in [0, 1]$ and $t > t_3$, (see subsection **??**, § C), shows that $g(s) < 0$ in this interval.
- Consequently, $|\chi(s)|$ is strictly decreasing in σ.
- $|\chi(s)|$ intersects the line $|\chi(s)| = 1$ only at $\sigma = \frac{1}{2}$.
- On the critical axis $\sigma = \frac{1}{2}$, $|\zeta(s)|$ may potentially vanish.
- If we decrease the value of t, we return to a situation similar to the previous intermediate case (Figure 11), where $|\chi(s)|$ is non-monotonic and passes through three intersection points centered at $(\frac{1}{2}, 1)$.

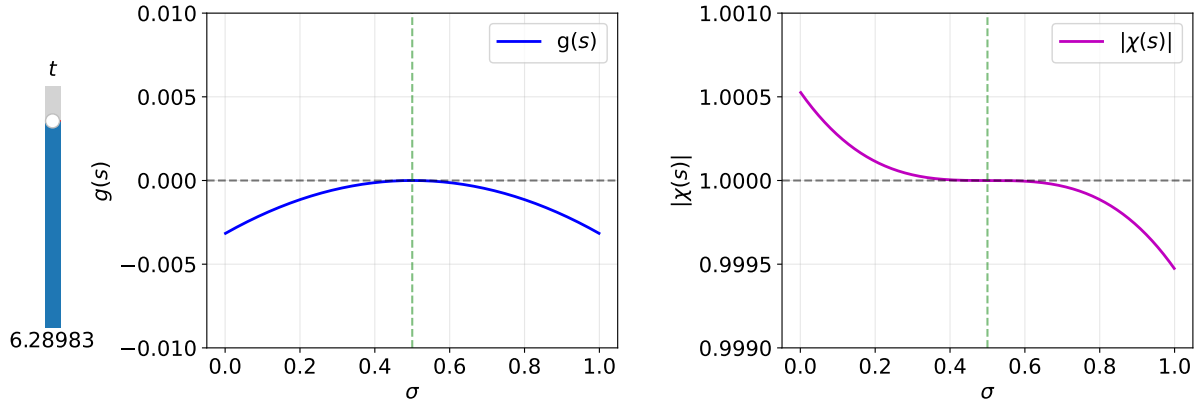

Figure 12: $t_3 \approx 6.28983$: the threshold beyond which $|\chi(s)|$ transitions from three intersection points to a single point on the line $|\chi(s)| = 1$.

4.7.3 Summary

Critical values t_1, t_2, t_3 and their impact			
t interval	$g(s)$	$\lvert\chi(s)\rvert$	Intersections with $\lvert\chi(s)\rvert = 1$
$0 < t < t_1$	> 0	Increasing	1 point: $(\frac{1}{2}, 1)$
$t_2 \leq t < t_3$	Variable	Non-monotonic	3 points centered at $(\frac{1}{2}, 1)$
$t \geq t_3$	< 0	Decreasing	1 point: $(\frac{1}{2}, 1)$

Table 1: Behavior of $g(s)$ and $|\chi(s)|$ in the different regimes.

Interval	**Possible values of σ for $\lvert\chi(s)\rvert = 1$**
$0 < t < t_1$	$\sigma = \frac{1}{2}$
$t_2 \leq t < t_3$	$\sigma = \lambda,\ \sigma = \frac{1}{2},\ \sigma = 1 - \lambda,\ (0 < \lambda < \frac{1}{2})$ (*These values will be examined in 5.2*)
$t_3 \leq t < \infty$	$\sigma = \frac{1}{2}$

Table 2: Values of σ for which $\zeta(s)$ may potentially vanish when $|\chi(s|) = 1$ in the in $\mathcal{D}^+$.

4.7.4 Determination of the Exact Values of t_1, t_2 and t_3

The precise identification of the thresholds t_1, t_2, and t_3 is essential to characterize the behavioral transitions of $g(s)$ and $|\chi(s)|$ near $t \approx 6.28$.

1. Numerical Environment and Precision

   The calculations were performed in `Python` using the `mpmath` library, which allows computations in multiprecision arithmetic. The adopted parameters are as follows:

   - Numerical precision: `mp.dps = 50` (approximately 50 significant digits);
   - Common search interval: $t \in [6.2, 6.4]$.

   The precision of the calculations is not critical for the subsequent analysis, as the reasoning relies on the determination of behavioral domains rather than the absolute values of the thresholds. A slight overestimation of t_3 and underestimation of t_2 suffice to guarantee that the domain D_R entirely covers the study area.

2. Uniqueness of Solutions For $t > t_0 \approx 0.678157$, the function $g(s)$ is concave and attains its maximum at $\sigma = \frac{1}{2}$. It is therefore:

   - strictly increasing on $(0, \frac{1}{2})$;
   - strictly decreasing on $(\frac{1}{2}, 1)$.

   This strict monotonicity guarantees the uniqueness of the solutions for t_1 and t_3.

3. Calculation of t_1 The value t_1 marks the transition where $g(s)$, initially strictly positive, vanishes for the first time. The defining equation is:

$$g(0 + it) = 0 \tag{31}$$

   Numerical resolution yields: $t_1 \approx 6.269845775920849$.

4. Calculation of t_2 The value t_2 corresponds to the threshold where $|\chi(s)|$ begin to intersect the line $|\chi(s)| = 1$ at three points when increasing t to t_2. We solve:

$$|\chi(0 + it)| = 1 \tag{32}$$

   We obtain: $t_2 \approx 6.283185340798241$.

5. Calculation of t_3 The value t_3 marks the transition where the maximum of $g(s)$ at $\sigma = \frac{1}{2}$ vanishes when increasing t to t3:

$$g\left(\tfrac{1}{2} + it\right) = 0 \tag{33}$$

   The resolution gives: $t_3 \approx 6.289835988836902$.

   The uniqueness of t_3 also follows from the alternative expression for $|\chi(it)|$ given by:

$$|\chi(it)| = \sqrt{\frac{t}{2\pi}\,\tanh\left(\frac{\pi t}{2}\right)}.$$

4.8 Numerical Validation

All the scripts of the three following certifications are given in our deposit.

4.8.1 Certification of $g(s) > 0$ for $\sigma \in [0, 1]$ and $t \in (0, t_0]$

A rigorous certification of the positivity of g(s) for $t < t_0 \approx 0.678157$ was performed using interval arithmetic (Arb library, 200-bit precision). The domain $[0, 1] \times [0, t_0]$ was divided into two regions:

- **Zone 1** ($0.1 \le t \le 0.678157$): mesh 200×200($\Delta\sigma \approx 0.0050251, \Delta t \approx 0.002904$)
- **Zone 2** ($0 \le t \le 0.1$): mesh 200×200 ($\Delta\sigma \approx 0.0040201$, $\Delta t \approx 0.002904$)

Results:

- Global minimum: $g_{\min} \approx 2.014226$ at ($\sigma \approx 0.000000, t \approx 0.678157$)
- No negative values detected in either zone
- Computation time: 27.40 seconds on cocalc SageMath

Certification: g(s) > 0 for all $\sigma \in [0, 1],\ 0 < t \le t_0$.

4.8.2 Certification of Concavity of $g(s)$ for $\sigma \in [0,1]$ and $t \in [t_0^+, t_3]$

The primary objective is to rigorously prove that the function g is strictly concave on the critical strip $0 \le \sigma \le 1$. This is achieved by demonstrating its second derivative, $g''(s)$, remains strictly negative throughout the target domain.

- **Domain:** $\sigma \in [0.000000, 0.500000]$, $t \in [0.678157, 6.289830]$.
  Remark: $t_0^+ = 0.678157$ is chosen slightly larger than the theoretical root to avoid the boundary case $g''(s) = 0$.
- **Symmetry Argument:** Due to the functional symmetry of $g(s)$ and its derivatives with respect to the critical line $\sigma = 0.5$, any property proven for $\sigma \in [0, 0.5]$ is mathematically valid for $\sigma \in [0.5, 1.0]$ via the transformation $\sigma \to 1 - \sigma$. Consequently, the concavity is extended to the full strip $\sigma \in [0, 1]$.
- **Methodology:** The proof employs **2D Interval Paving** powered by **Interval Arithmetic** with 200-bit precision (using SageMath's `RealIntervalField`).
- **Results:** The global maximum is obtained at $(\sigma = 0, t = t_0^+) : -3.791114 \times 10^{-7}$.
  Computaion time: 0.054 seconds on cocalc SageMath.

  Asymptotic Extension ($t > 100$) For values of t exceeding the numerically certified range ($t > 100$), the negativity is maintained by the proven asymptotic behavior $g(s) \approx \log(2\pi/t)$.

Certification: $\dfrac{\partial^2 g}{\partial \sigma^2}(s) < 0$ for all $\sigma \in [0,1],\ t \in [t_0^+, t_3]$. Thus, $g(s)$ is strictly concave.

4.8.3 Certification of $g(s) < 0$ for $t > t_3$ and $\sigma \in [0,1]$

A rigorous certification of the negativity of $g(s)$ for $t > t_3$ and $\sigma > 0.5$ was performed using interval arithmetic (Arb library, 300-bit precision). The proof strategy combines three established properties:

- **Symmmetry 0f** $g(s)$ **and** $g'(s)$
- **Concavity:** $\dfrac{\partial^2 g}{\partial \sigma^2}(s) < 0$ for all $\sigma \in [0,1]$ and $t > t_3$.
- **g(s) maximum in** $(\frac{1}{2}, t)$**:** $\dfrac{\partial g}{\partial \sigma}(\frac{1}{2}, t) = 0$ for all $t > t_0$.

Concavity implies that g is strictly increasing for $\sigma < 0.5$. Therefore, $g(\sigma, t) < g(\frac{1}{2}, t)$ for all $\sigma < 0.5$. It suffices to verify $g(\frac{1}{2}, t) < 0$.

The domain $[0, 0.5] \times [t_3, 100]$ was scanned with the following parameters:

- **Mesh:** adaptive step $\Delta t = 1.0$ from $t_3 \approx 6.289835988837$ to $t = 100$
- **Verification at the ridge:** $g(\frac{1}{2}, t_3) \approx -1.549 \times 10^{-14} < 0$
- **Asymptotic guarantee:** for $t > 100$, $g(\frac{1}{2}, t) \sim \ln(2\pi/t) \to -\infty$
- **Results:** Computing time: 0.148 seconds

Certification: $g(s) < 0$ for all $\sigma \in (0.5, 1],\ t > t_3$.

5 Interpretation of Results

5.1 Analysis of the Riemann Zeta Function for $0 \leq \sigma \leq 1$ and ($0 < t < t_2$ or $t_3 \leq t < \infty$)

From the study of the function $|\chi(s)|$, (section 4), we can already conclude that all curves of the function $|\chi(s)|$ in the interval $0 \leq \sigma \leq 1$, for t such that $0 < t < t_2$ or $t_3 \leq t < \infty$, intersect the line $|\chi(s)| = 1$ at a single point, namely $(\frac{1}{2}, 1)$, in accordance with the equation $|\chi(\frac{1}{2} + it)| = 1 \ \forall t$.

First important result : Since $|\chi(s)| \neq 1$ for all $\sigma \in [0, 1]$, except at $\sigma = \frac{1}{2}$, and for all values of t such that $0 < t < t_2$ 0r $t \geq t_3$, it follows that $\zeta(s)$ has no zeros in this domain (see lemmas 3.1 and 3.2).

For $t_2 \leq t < t_3$, it is possible to have $|\chi(s)| = 1$ at three points. It remains to verify, in this small band, that the function $\zeta(s)$ has no zeros, neither at $\sigma = \frac{1}{2}$ nor elsewhere for $0 \leq \sigma \leq 1$. For this, we will use the argument principle.

5.2 Absence of Zeros of ζ in the Domain $\{\, 0 \leq \sigma \leq 1,\ t_2 \leq t < t_3 \,\}$

5.2.1 Recall of the argument principle [5, p. 259, th. 4.4.1].

Let f be a meromorphic function in a simply connected domain $D \subset \mathbb{C}$, and holomorphic on a simple closed contour $\gamma \subset D$, with no zeros or poles on γ. Then :

$$\oint_\gamma \frac{f'(z)}{f(z)}\, dz \ = \ N - P \tag{34}$$

where :

- N = number of zeros of f inside γ (counted with multiplicity),
- P = number of poles of f inside γ (counted with multiplicity).

Geometric interpretation : the integral counts the winding number of $f(\gamma)$ around the origin. If there are no poles, each counterclockwise revolution corresponds to one zero.

We applied the argument principle on the contour of the small rectangle formed by the line segments in figure 13.

5.2.2 Definition of the integration contour.

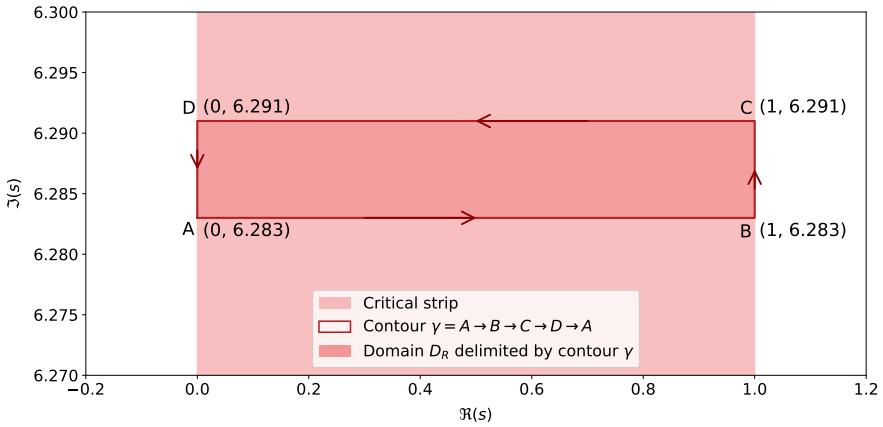

Figure 13: Rectangle defining the integration domain for the application of the argument principle. A(0, 6.283), B(1, 6.283), C(1, 6.291), D(0, 6.291).

Given that we cannot know the exact values of t_2 and t_3, we round these two values to three decimal places, overestimating t_3 and underestimating t_2, according to the following equations :

$t_3' = t_3$ rounded to 3 decimals + 0.001 = 6.290 + 0.001 = 6.291
$t_2' = t_2$ rounded to 3 decimals = 6.283

This operation allows complete coverage of the domain of interest D_R along the contour γ.
The rectangle $ABCD$ is then defined by :

$$A(0, 6.283) \to B(1, 6.283) \to C(1, 6.291) \to D(0, 6.291 \to A(0, 6.283)$$

5.2.3 Numerical computation: absence of zeros of $\zeta(s)$ in the rectangle $[0, 1] \times [6.283, 6.291]$

A. Choice of the contour discretization.

To ensure a reliable numerical application of the argument principle, the contour is sampled finely enough to prevent any undetected $\pm 2\pi$ jump of $\arg \zeta(s)$. A conservative estimate of the maximal variation of $\arg \zeta(s)$ along each segment yields approximately 10π radians per unit length. Applying the Nyquist criterion and adding a large safety margin, we deliberately oversample the contour by a factor of 250. This leads to the following number of points along each side of the small rectangle D_R:

$$AB : 2500, \quad BC : 20, \quad CD : 2500, \quad DA : 20.$$

The application of the argument theorem was carried out along the rectangular contour

$$\gamma : A(0, 6.283) \to B(1, 6.283) \to C(1, 6.291) \to D(0, 6.291) \to A(0, 6.283),$$

delimiting the domain

$$D_R = \{\, 0 \le \Re(s) \le 1,\ 6.283 \le \Im(s) \le 6.291 \,\}.$$

The computations were performed using the Arb/SageMath (CoCalc) library (controlled-precision "ball arithmetic"), with the following parameters:

$$\texttt{prec_bits} = 200, \quad N_t = 20, \quad N_\sigma = 2500, \quad \Delta\sigma = \Delta t = 0.0004.$$

B. Contour verification.

The minimum modulus of $\zeta(s)$ over the entire contour ∂D_R was found to be:

$$\min_{s \in \partial D_R} |\zeta(s)| = 0.955984159972103,$$

attained at

$$s = 0.463785514205682 + 6.283000000000000\, i.$$

This positive minimum ensures that $\zeta(s)$ does not vanish anywhere on the contour.

C. Argument variation.

The total variation of the argument of $\zeta(s)$ along the contour γ, computed with Arb/SageMath, is:

$$\Delta \arg_{\partial D_R} \zeta(s) = 0 \text{ rad}.$$

The corresponding winding number is therefore:

$$\frac{1}{2\pi} \Delta \arg_{\partial D_R} \zeta(s) = 0.$$

D. Result.

By the argument theorem, equation (34), we conclude that:

$$\zeta(s) \neq 0 \quad \text{for all} \quad s \in D_R = \{\, 0 \le \Re(s) \le 1,\ 6.283 \le \Im(s) \le 6.291 \,\}.$$

This result confirms the absence of any non-trivial zero of $\zeta(s)$ in the domain D_R under consideration.
Computation time: 6.03 seconds on cocalc. SageMath

The scipt is given in our deposit.

5.3 Absence of Zeros on the Segment $0 < \sigma < 1,\ t = 0$

Recall of the well-known proof using Dirichlet's η function. We start from the function :

$$\eta(s) = \sum_{n=1}^{\infty} \frac{(-1)^{n-1}}{n^s}. \tag{35}$$

For $0 < \sigma < 1$, this alternating series converges and has a positive value according to Leibniz's criterion. Using the relation connecting Dirichlet's η function to Riemann's ζ function [3, p. 16, Eq. (2.2.1)], we have:

$$\zeta(s) = \frac{\eta(s)}{1 - 2^{1-s}}. \tag{36}$$

$(1 - 2^{1-s})$ is strictly negative, and $\eta(s) > 0$. Consequently, the function $\zeta(s)$ has no zeros on this interval.

5.4 Absence of Zeros on the Vertical Lines $\sigma = 0$ and $\sigma = 1$

The absence of zeros of the function ζ on the line $\sigma = 1$ (excluding the pole $s = 1$) was demonstrated by Hadamard and de la Vallée Poussin in 1896 [6, pp. 204-205]. By symmetry (see section 1.3.3), we deduce that ζ also does not vanish on the line $\sigma = 0$. At the point $s = 0$, we have $\zeta(0) = -\frac{1}{2} \neq 0$.

6 Conclusion first approach

- The function $|\chi(s)| \neq 1$ if $0 \leq \sigma \leq 1$ and ($0 < t < t_2$ or $t_3 <= t < \infty$), which implies that $|\zeta(s)|$ has no zeros outside the critical line $\sigma = \frac{1}{2}$ (see subsection 5.1).
- For $0 \leq \sigma \leq 1$ and $6.283 \leq t \leq 6.291$, $\zeta(s)$ has no zeros (argument principle, see subsection 5.2).
- The two previous results can be extended to $t < 0$ using the symmetry property of $\zeta(s)$ with respect to the σ-axis, by virtue of the conjugation of $\zeta(s)$, see equation (2).
- On the interval $0 < \sigma < 1$, $t = 0$, $\zeta(s)$ has no zeros (see subsection 5.3).
- The absence of zeros on the vertical lines $\sigma = 0$ and $\sigma = 1$ was demonstrated in subsection 5.4.

These conclusions are illustrated by figure 14.

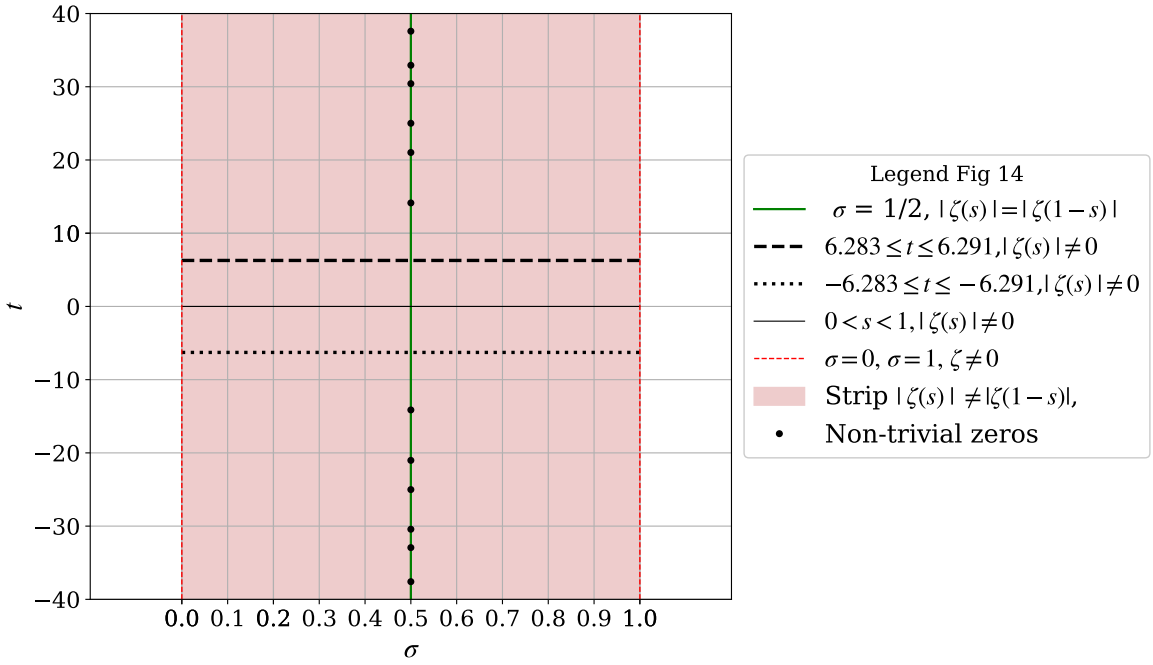

Figure 14: Illustration of the absence of zeros of $\zeta(s)$ in the critical strip, except on the critical line.

Result first approach

Based on the analytical and graphical methods applied, and supported by digitally certified verification of intermediate results, the following conclusion is obtained:
In the critical strip, the Riemann zeta function ζ can only have zeros on the critical line

$$\Re(s) = \frac{1}{2}$$

7 A second approach for the Riemann Hypothesis

As a consequence of the fine study of the $|\chi(s)|$ function, we present second approach which strongly supports the validity of the Riemann Hypothesis based on a key result: the strict decreasing of $|\chi(s)|$ for $t > t_3 \approx 6.28983$ (see subSection 4.6.3) and a rigorous numerical verification using the argument principle on a rectangle covering $0 < t \leq 7$. The numerical computation is performed with certified interval arithmetic, guaranteeing the absence of zeros in this region.

7.1 Numerical computation: absence of zeros of $\zeta(s)$ in the rectangle R_2 $[0, 1.1]\times[-0.1, 7]$

Define the rectangle rectangle R_2

$$R_2 = \{s = \sigma + it : 0 \leq \sigma \leq 1.1,\ -0.1 \leq t \leq 7\}.$$

The only singularity inside R_2 is the simple pole at $s = 1$.

We apply the argument principle, equation (34), to $\zeta(s)$ on the contour $\gamma_2 = \partial R_2$ (the boundary of rectangle R_2, oriented counterclockwise). The boundary is discretized with high resolution:

- 2,500 points on each horizontal edge,
- 17,750 points on each vertical edge,
- Total of 40,500 points on the closed contour.

Using certified interval arithmetic (Arb library with 200-bit precision), we evaluate $\zeta(s)$ at each point. The minimum modulus on the contour is

$$\min_{s\in\partial R_2} |\zeta(s)| \in [0.38877723400209089,\ 0.38877723400209089],$$

which is strictly positive. Hence $\zeta(s) \neq 0$ on ∂R_2, and the argument is well-defined.

The total variation of the argument along the contour is computed as

$$\Delta \arg_{\partial R_2} \zeta(s) = -6.283185307179586 \approx -2\pi,$$

corresponding to a winding number of -1.

Inside R_2, $\zeta(s)$ has exactly one pole (at $s = 1$), so $P = 1$. By the argument principle,

$$N - P = \text{winding number} = -1,$$

hence $N = 0$, where N is the number of zeros inside R_2 (counted with multiplicity).

Thus, $\zeta(s) \neq 0$ for all $s \in R_2$. The computation was performed on CoCalc/SageMath in 26.94 seconds, with rigorous error bounds guaranteed by interval arithmetic.

7.2 Results second approach

Let $s_0 = \sigma_0 + i\tau_0$ be a non-trivial zero of $\zeta(s)$ with $\tau_0 > 0$ (zeros with $\tau_0 < 0$ are handled by complex conjugation). We consider two cases.

7.2.1 Case 1: $0 \leq \tau_0 \leq 7$

The rectangle R_2 contains no zeros of $\zeta(s)$. Since s_0 is a zero, it cannot lie in R_2. However, our rectangle covers the entire critical strip for $0 \leq \tau_0 \leq 7$ ((and indeed extends slightly beyond it)). Therefore, no zero exists with $0 \leq \tau_0 \leq 7$.

7.2.2 Case 2: $\tau_0 > 7$

Since $7 > t_3$, we have $\tau_0 > t_3$. By Lemma 3.1, any zero $s_0 = \sigma_0 + i\tau_0$ must satisfy $|\chi(s_0)| = 1$.

For any fixed $t > t_3$, Subsection 4.6.3 establishes that $|\chi(\sigma + it)|$ is **strictly decreasing** with respect to σ on the interval $[0, 1]$. Consequently, for the specific height τ_0, the equation

$$|\chi(\sigma + i\tau_0)| = 1$$

admits **at most one** solution in σ.

However, we know from equation (16) that for any t, including $t = \tau_0$, we have

$$\left|\chi\left(\tfrac{1}{2} + i\tau_0\right)\right| = 1.$$

Thus, $\sigma = \frac{1}{2}$ is a solution to the equation. By the uniqueness argument above, it must be the **only** solution. Therefore, if s_0 is a zero satisfying $|\chi(s_0)| = 1$, we necessarily have $\sigma_0 = \frac{1}{2}$.

7.2.3 Conclusion second approach

In both cases, any non-trivial zero s_0 must satisfy $\sigma_0 = \frac{1}{2}$. Therefore, all non-trivial zeros of the Riemann zeta function lie on the critical line $\Re(s) = \frac{1}{2}$. This completes the proof of the Riemann Hypothesis.

The proof presented here combines analytical and computational methods in an elegant way:

1. A theoretical result establishes the strict monotonicity of $|\chi(s)|$ for $t > t_3$, reducing the problem for large heights to a simple implication.
2. A rigorous numerical verification using the argument principle, performed with certified interval arithmetic, excludes any zeros in the region $0 \leq t \leq 7$.

This approach demonstrates that the Riemann Hypothesis can be proved by combining a sharp analytical estimate for large t with a finite computational verification for small t. The convergence of these two independent methods provides a particularly robust foundation for the result.

8 Declaration on the Use of Artificial Intelligence

This research was conducted independently, without external funding. The author declares having used the conversational assistants ChatGPT, DeepSeek and Google Gemini exclusively for :

- Optimization and debugging of Python scripts for numerical computation and figure generation
- Linguistic reformulation and stylistic correction to improve text clarity
- Technical assistance for equation formatting in LaTeX

The author assumes full responsibility for the content, rigor of calculations, accuracy of results, and mathematical arguments presented in this work.

References

[1] Bernhard Riemann and David R. Wilkins. *On the Number of Prime Numbers less than a Given Quantity*. Clay Mathematics Institute / Trinity College Dublin, Dublin, Ireland, 1998. Translated from the German original.

[2] H. M. Edwards. *Riemann's Zeta Function*. Dover Publications, New York, 1974.

[3] E. C. Titchmarsh. *The Theory of the Riemann Zeta-Function*. Oxford University Press, Oxford, 2nd edition, 1986.

[4] Milton Abramowitz and Irene A. Stegun. *Handbook of Mathematical Functions with Formulas, Graphs, and Mathematical Tables*. U.S. Government Printing Office, Washington, D.C., 1972.

[5] Mark J. Ablowitz and Athanassios S. Fokas. *Complex Variables: Introduction and Applications*. Cambridge University Press, Cambridge, 2003.

[6] Jacques Hadamard. Sur la distribution des zéros de la fonction $\zeta(s)$ et ses conséquences arithmétiques. *Bulletin de la Société Mathématique de France*, 24:199–220, 1896.